



Rules and Exceptions: The Role of Chromosomal ParB in DNA Segregation and Other Cellular Processes

Adam Kawalek †, Paweł Wawrzyniak †, Aneta Agnieszka Bartosik and Grazyna Jagura-Burdzy *

Institute of Biochemistry and Biophysics, Polish Academy of Sciences, Department of Microbial Biochemistry, Pawińskiego 5a, 02-106 Warsaw, Poland; a.kawalek@ibb.waw.pl (A.K.); wawrzyniakp@ibb.waw.pl (P.W.); anetab2@ibb.waw.pl (A.A.B.)

* Correspondence: gjburdzy@ibb.waw.pl; Tel +48-225921212

† These authors contributed equally to this work

Received: 4 December 2019; Accepted: 9 January 2020; Published: 11 January 2020

Abstract: The segregation of newly replicated chromosomes in bacterial cells is a highly coordinated spatiotemporal process. In the majority of bacterial species, a tripartite ParAB-*parS* system, composed of an ATPase (ParA), a DNA-binding protein (ParB), and its target(s) *parS* sequence(s), facilitates the initial steps of chromosome partitioning. ParB nucleates around *parS*(s) located in the vicinity of newly replicated *oriC*s to form large nucleoprotein complexes, which are subsequently relocated by ParA to distal cellular compartments. In this review, we describe the role of ParB in various processes within bacterial cells, pointing out interspecies differences. We outline recent progress in understanding the ParB nucleoprotein complex formation and its role in DNA segregation, including *ori* positioning and anchoring, DNA condensation, and loading of the structural maintenance of chromosome (SMC) proteins. The auxiliary roles of ParBs in the control of chromosome replication initiation and cell division, as well as the regulation of gene expression, are discussed. Moreover, we catalog ParB interacting proteins. Overall, this work highlights how different bacterial species adapt the DNA partitioning ParAB-*parS* system to meet their specific requirements.

Keywords: ParB; segrosome; chromosome segregation; cell division; gene expression regulation; partitioning proteins

1. Introduction

Bacterial genomes consist of circular or linear and single or multiple chromosomes as well as extra-chromosomal elements like plasmids. They are highly compact spatially and temporally organized entities [1–4]. Chromatin organization is linked to processes such as DNA replication and chromosome segregation and transcription [1,5–9]. In dividing cells, a bi-directional, semi-conservative replication initiated from *oriC* proceeds simultaneously with the segregation of compacted daughter nucleoids. Specific factors, such as DNA supercoiling, and proteins, such as nucleoid associated proteins (NAPs), determine, maintain, and modify the spatial organization of bacterial nucleoids during the entire cell cycle, from the initiation of replication to the end of the division cycle (reviewed in [2,10–12]).

Bacterial genomes are divided into macrodomains 0.5–1.5 Mbp in size, with the *ori* domain (up to 20% of the genome around the origin of replication *oriC*) and *ter* domain (part of the chromosome around the terminus of replication) playing pivotal roles [13–18]. A chromosome interaction map constructed for *Caulobacter crescentus* revealed that its genome is additionally split into 23 self-

interacting regions of 30–400 kbp, designated chromosome interacting domains (CID) [9]. A similar number of CIDs ranging in size from 50 to 300 kbp were identified in the *Bacillus subtilis* genome [16]. The boundaries of CIDs frequently co-localize with highly transcribed genes [9,19–22]. The role of NAPs in chromosomal long- and short-range interactions [4,23,24] and among them, the structural maintenance of chromosome proteins (SMCs and MukBs) [25–28], has been widely documented. In *Mycoplasma pneumoniae*, 10–15 kb microdomains with similar gene expression patterns were identified [29].

Chromosomes in most rod-like bacteria, including *B. subtilis*, *C. crescentus*, *Pseudomonas aeruginosa*, *Vibrio cholerae*, and *Myxococcus xanthus*, adopt longitudinal organization. In this arrangement, the two replication arms align along the long axis of the cell, whereas the *ori* and *ter* domains locate at opposite cell ends [9,16,28,30,31]. The left and right arms are thought to wrap around each other, leading to a juxtaposition of the corresponding fragments of opposite chromosome arms [32–34]. The *Escherichia coli* chromosome exemplifies a transversal configuration, with the *ori* and *ter* localized in the middle of the cell and the two replication arms occupying distinct cell halves [17,35,36]. The dynamic and species-specific movements of particular chromosomal regions suggest that different factors may be involved in their organization and spatiotemporal segregation.

In this review, we summarize our current understanding of chromosomal ParAB-*parS* partition systems, which are involved in *ori* positioning in many species. We focus on the diverse roles of the ParB component and present recent advances in the ParB nucleoprotein complex formation, its involvement in DNA segregation, and other more specialized functions. Moreover, we catalog ParB interacting proteins from various species, which indicates that the biological roles of ParAB-*parS* systems may extend far beyond the chromosome segregation process.

2. ParAB-*parS*-Driven DNA Segregation—from Plasmids to Chromosomes

The accurate distribution of genetic material in bacteria was initially studied for low-copy-number plasmids, which secure their maintenance in the bacterial population by active DNA partition processes [37–40]. The vast majority of such plasmids uses three component Par systems built from an operon encoding an NTPase (A component, “motor protein”) together with a DNA-binding protein (B component), as well as *parS*, a centromere-like DNA sequence [41–43]. NTPases belong to Walker-type ATPases (partition system of Class I, ParA superfamily) [44,45], actin-like ATPases (Class II) [46], or tubulin-like GTPases (Class III) [47]. The B components use either helix-turn-helix (HTH) (ParB family) [48–51], ribbon-helix-helix (RHH) [52–54], or winged HTH motifs [55] for DNA binding to *parS*: specific inverted or direct sequence repeats occurring in a single or multiple copies in the plasmid genomes. Despite the structural variability of ParAB-*parS* elements between plasmids, the main steps of active plasmid partition are conserved. The B component specifically binds to *parS* site(s) and forms a nucleoprotein complex called a segrosome. The segrosome attracts NTPase, which, in turn, actively separates segrosome pairs by moving individual segrosomes towards the poles of dividing cells [56]. This cellular localization assures that each progeny cell will obtain at least one copy of the plasmid DNA (reviewed in [15,57]).

Studies on plasmid partition received special attention when the sequencing of bacterial genomes revealed *oriC* proximal operons encoding Class Ia plasmidic orthologs, ParAs, Walker-type ATPases, and ParBs, large proteins with a central HTH motif [41,58–60]. The third element, the variable plasmid-specific sequence(s), are replaced by a highly conserved palindromic *parS*s, mainly TGTTCACGTGAAACA, present in varying numbers in the vast majority of single chromosomes, as well as the primary chromosomes of multipartite bacterial genomes (Table 1). To date, *par* genes have not been found in the chromosomes of the two families of γ -proteobacteria, *Enterobacteriaceae* (e.g., *E. coli*) and *Pasteurellaceae* (e.g., *Haemophilus influenzae*), or in one family of Mollicute, *Mycoplasmataceae* (e.g., *Mycoplasma* sp). Moreover, a few species seem to miss particular *par* elements (e.g., *Streptococcus pneumoniae* lacks *parA*) [41,59].

The homology between the chromosomal and low-copy-number plasmid counterparts of ParA and ParB families implicates their participation in DNA segregation. Indeed, chromosomal *par*

operons accompanied by a single *parS* site from the same genome were shown to stabilize otherwise unstable plasmids and Par proteins were able to correctly position the plasmids even within heterologous host cells [61–64]. Undoubtedly the chromosome segregation process faces more spatiotemporal challenges than the partition of small plasmid genomes.

The segregation of simultaneously replicating chromosomes proceeds in a few stages. The newly duplicated *ori* domains are re-folded and pushed away, directed, and held at certain cellular positions. The bulk of chromosome arms follows them, and finally, the *ter* domains become physically separated [2,65–67]. Studies on the role of ParAB-*parS* systems have revealed their engagement in *ori* domain compaction, directional movements, and specific positioning in the cell until cell division (Figure 1), in a species-specific manner. These systems are indispensable in some species, such as *C. crescentus* or *M. xanthus*, and are an accessory in the majority of other species (Table 1).

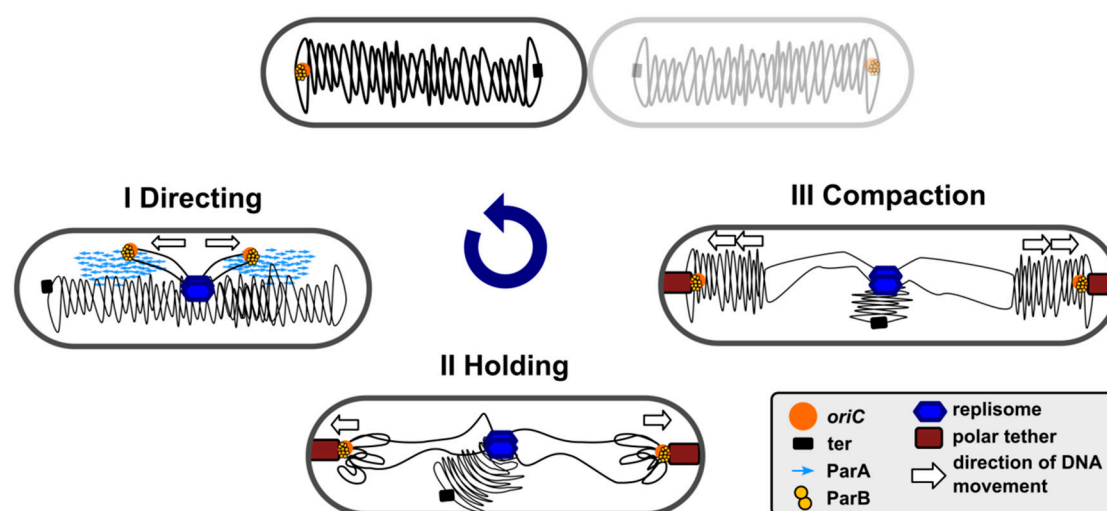


Figure 1. Involvement of partition ParB protein in *ori* domain re-locations, structuring and positioning during bacterial cell cycle. A simplified scheme for *P. aeruginosa*-like longitudinal chromosome rearrangements is presented, in which the replisome is located in the cell centre, and the ParB-bound *ori* domains are anchored close to the cell poles before division [30].

1

Table 1. Characterization of chromosomally encoded *par* systems.

Species	<i>parS</i> Sites Total / in ori Domain/ Consensus	<i>par</i> Genes	Anucleate Cells in <i>parB</i> Mutant	Other Phenotypes associated with Mutation in <i>parB</i> Gene
Gram-positive:				
Firmicutes				
<i>Bacillus subtilis</i>	10 / 8 / TGTTNCACGTGAAACA [68]	non-essential	1%–2% (wt 0.02%) [69]	Defect in sporulation, elongated cells, increased amount of DNA <i>per</i> cell, overreplication: >2 foci corresponding to <i>ori</i> in 35.4% cells (wt 15.3%), disturbed replication control and <i>ori</i> separation [70], impaired SMC loading (lack of foci) [6]
<i>Streptococcus pneumoniae</i>	4 / 4 / AGTTTCACGTGAAACT [71]	non-essential, no <i>parA</i>	0.8% at 30 °C to 3.5% at 37 °C (wt 0%) [71]	No apparent growth defects, mild perturbations in chromosome segregation, decreased SMC loading near origin [71]
Actinobacteria				
<i>Corynebacterium glutamicum</i>	10 / 10 / TGTTNCACGTGAAACA [72]	non-essential	43.8% in MMI medium, 11.6% in LB (wt 0%) [73]	Reduced growth rate in MMI medium, growth not affected in an LB medium, altered cell morphology (almost “coccoid” cells and elongated anucleate cells) [73], impaired SMC loading (lack of visible foci) [72]
<i>Mycobacterium smegmatis</i>	3 / 3 / GTTTCACGTGAAAC [74]	non-essential	10.3% (wt 0.8%) [74]	Elongated cells, overreplication, disturbed septa formation, origin positioning, and chromosomal topology [75]
<i>Streptomyces coelicolor</i>	21 / 21 / tGTTTCACCTGAAACa [76]	non-essential	13%–17.4% anucleate spores (wt 1%–2%) [77,78]	Disturbed sporulation, reduced growth rate, elongated cells, premature and irregular Z-ring formation [79]
Gram-negative:				
Alphaproteobacteria				
<i>Caulobacter crescentus</i>	5 / 5 / t/cGTTt/cCACGTGAAACa [80,81]	essential		Indispensable, severe chromosome segregation defects, ParB depletion results in defective Z-ring formation and cell division, formation of long polyploid cells [82]
<i>Hyphomonas neptunium</i>	2 / 2/ TGTTTCACGTGAAACA [83]	essential	anucleate buds [83]	<i>parB</i> mutants could not be obtained, depletion of ParA blocks cell division [83]
Betaproteobacteria				
<i>Burkholderia cenocepacia</i>	chrI: 2 / 2 / tGTTNCACGTGAAACa chrII: 6 / 6 / gTTTATGCGCATAAAc [84–87]	non-essential	1–14% (depending on mutated system) [85]	Reduced growth rate, reduction in cell size, compromised viability, defects in ori positioning [85]

Deltaproteobacteria				
<i>Myxococcus xanthus</i>	22 / 22 / TGTTCCACGTGGAACG [88]	essential	ParB depletion: 1% after 24 h, 10.1–21.6% after 36–48 h [88]	ParB depletion: aberrant cell morphology, anomalies in DNA segregation and cell death [88]
Gammaproteobacteria				
<i>Pseudomonas aeruginosa</i>	9 / 4 / TGTTCCACGTGGAACa half- <i>parSs</i> GTTCCAC or GTTTCAC [89–91]	non-essential	2–4% in LB medium, to 7% in an M9 medium (wt < 0.01%) [92]	Reduced growth rate, 10–15% increase in cell size and 10% longer generation time, altered colony morphology, affected motility; decreased ParA stability [92]
<i>Pseudomonas putida</i>	?* / 3 TGTTCCACGTGGAACA [63]	non-essential	5–10% in minimal medium during the transition from exponential to stationary phase [93]	Defects in chromosome partitioning, abnormal cell morphologies during the deceleration phase of growth independent of the medium used [63,93]
<i>Vibrio cholerae</i>	chrI: 3 / 3 / NGTTNCACGTGAAACN chrII: 10 / 9 / NTTTACANTGTAAAN [94]	non-essential chr1 essential chr2	no change in <i>parB1</i> mutant [95]	Increased frequency of replication initiation, disturbed ori positioning in cell poles [95], no segregation defect for <i>V. cholerae</i> chrI [94]
Deinococci				
<i>Deinococcus radiodurans</i>	chrI: 3 / 1 / NGTTTcgcGtgaAACN [96]	non-essential	8%–13% for $\Delta parB1$, (wt >1%) [96]	Reduced growth rate for $\Delta parB1$ [96]
<i>Thermus thermophilus</i>	1 / 1 / TGTTTCCCGTGAAACA [97]	non-essential	3% for $\Delta parAB$ (wt 1.2%) [97]	No apparent growth defects for $\Delta parAB$ [97,98]

- 2 **Abbreviations:** *chrI/chrII*- primary/ secondary chromosome in the multipartite genome; **wt**—wild-type; ?* - only contig with *P. putida oriC* was
3 analyzed for presence of *parSs* in the cited reference.

4 Sequence analysis revealed that the vast majority of the ParA homologs encoded in the
5 chromosomes of Gram-negative and Gram-positive bacteria, as well as Archaea, cluster in a
6 subgroup, distinct from the groups of plasmidic Class Ia ParAs [41]. Chromosomal ParAs lack the N-
7 terminal DNA binding domain, present in plasmidic orthologs and required for autoregulation of
8 the cognate *par* operon [99,100].

9 Chromosomal ParAs, like their plasmidic counterparts of Class I, are Walker-type ATPases
10 capable of non-specific DNA binding [101,102] and interactions with cognate ParBs [64,103–105].
11 After ATP binding, chromosomal ParAs associate non-specifically with the nucleoid. ATP hydrolysis
12 stimulated by interactions with ParB bound to *parS*s triggers dynamic re-locations of the *oriC*
13 domains. Several models have been offered to explain the molecular mechanisms used by the ParAs
14 of Class I to move the ParB-*parS* complex towards the poles, including “pulling” [42,103,106–108],
15 “diffusion-ratchet”, and “DNA-relay” [109–111] and these mechanisms are still being discussed (for
16 a review, see [15,112,113]).

17 Eubacterial chromosomal ParBs (but not archaeal), and plasmid encoded Class Ia partition
18 proteins [41], belong to the ParB family. Chromosomal ParBs cluster together and show a much
19 higher conservation in their clade than more divergent plasmidic ParBs. Despite their apparent
20 diversity, all Class Ia ParBs share a similar domain and functional organization (Figure 2a). The
21 central DNA binding domain (DBD) with an extended HTH motif is connected by flexible linkers,
22 with the N-terminal oligomerization and ParA binding domain (NTD) containing the highly
23 conserved arginine patch, GERRxRA [114–117] (reviewed in [118]), and the C-terminal dimerization
24 domain (CTD) encompassing a leucine zipper [64,116,119]. Additionally, in some systems, CTD may
25 be involved in nonspecific DNA interactions (e.g., *B. subtilis* ParB homolog, designated Spo0J) [119–
26 121].

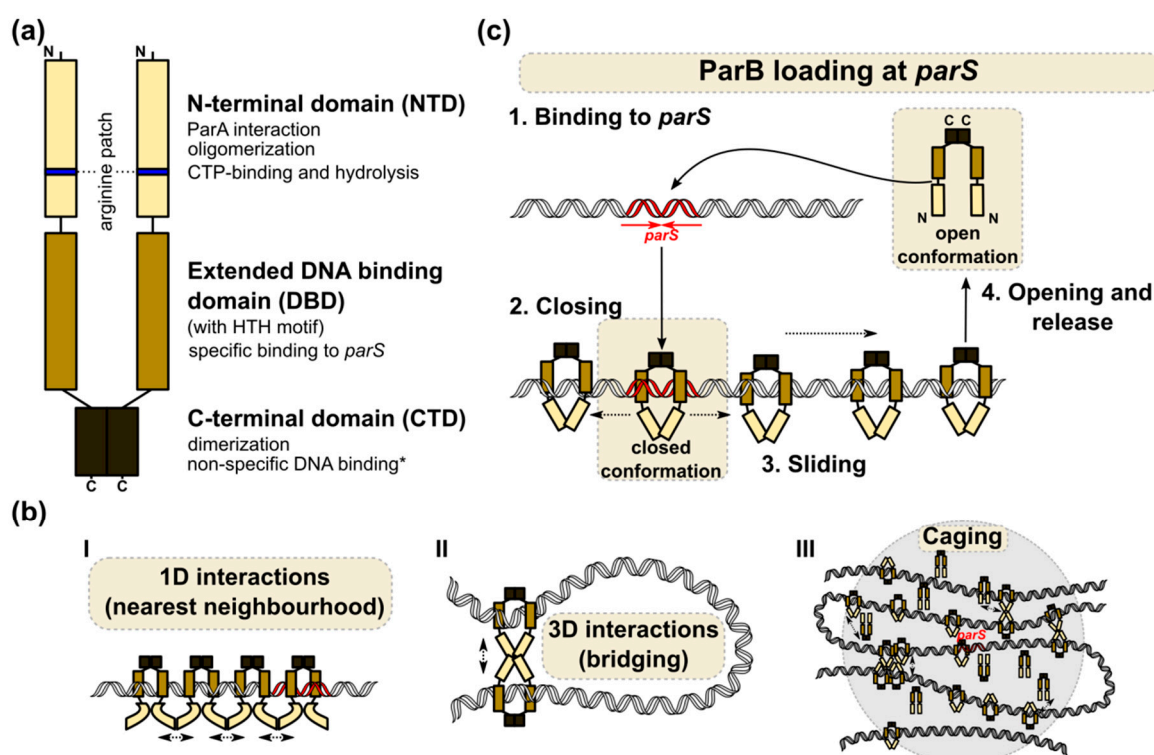


Figure 2. ParB complex assembly at *parS*. (a) Schematic representation of chromosomally encoded ParB protein (dimer) with the indicated functions of individual domains. *- only confirmed for *B. subtilis* Spo0J. (b) Models of the ParB-ParB interactions involved in formation of the ParB nucleoprotein complexes around *parS*. (I) Adjacent ParB dimers may interact with each other to form 1D filaments around *parS*. (II) Interactions between ParB dimers associated with distal DNA fragments may lead to DNA bridging and looping. (III) ParB self-interactions provide a scaffold (cage), attracting and trapping additional ParB

35 molecules. (c) A model illustrating ParB loading at *parS* and sliding [122]. Free CTP-ParB
 36 exists as a dimer in an open conformation. Binding to *parS* induces conformational changes
 37 involving the N-terminal ParB domains and the formation of “closed” ring-shaped
 38 molecules. Steric hindrance between HTH motifs interacting with *parS* in such a closed
 39 conformation may prompt the release of ParB rings from *parS* via their sliding on adjacent
 40 DNA and the loading of new ParB dimers at *parS*. Finally, switching from a closed to open
 41 conformation by an unknown mechanism (possibly involving CTP hydrolysis) may lead to
 42 ParB’s dissociation from the DNA. The *parS* sites are indicated in red.

433. The Structure of the ParB–*parS* Complex

44 Similarly to their plasmidic orthologs [123–126], chromosomal ParBs have a very unusual
 45 feature: after binding to *parS* as dimers, they spread on adjacent DNA [64,68]. It was shown that ParBs
 46 defective in spreading were impaired in partition [68,114,127].

47 ParB nucleation around the *parS* sequence correlates with the formation of ParB foci in
 48 fluorescence microscopy analyses [76,92,97,117,127–131] or the presence of wide peaks (up to 50 kbp),
 49 encompassing *parS* in chromatin immunoprecipitation analyses (ChIP-seq or ChIP-microarray),
 50 indicating the incorporation of *parS* proximal DNA in the ParB complex [68,71,72,79,80,89,90,129,132].

51 A combination of biochemical, structural, and computational approaches can shed light on the
 52 possible architecture of the ParB–*parS* nucleoprotein complex (reviewed in [118]). Nevertheless, no
 53 common assembly mechanism has been proposed, thus suggesting dynamic and heterogeneous
 54 interactions between ParB molecules within the complex (Figure 2b) [116,122,133,134]. It is widely
 55 acknowledged that ParB loading on *parS* is a prerequisite for the conformational changes that prime
 56 ParB for nucleation [135–137]. The ability of ParBs to build large nucleoprotein complexes may be a
 57 result of lateral ParB interactions (1D) and bridging interactions (3D) between ParB molecules located
 58 at distant DNA segments [117,134], clustering or building a ParB cage around *parS* by weak but
 59 dynamic interactions between protein dimers and DNA [129,138,139]. The ParB interactions around
 60 *parS* result in significant DNA compaction via loop formation. Interestingly, non-specific DNA
 61 binding also seems to be an important factor in DNA bridging and condensation, at least in some
 62 systems [120,121]. All models postulate that multiple ParB–ParB interaction interfaces must be
 63 involved in the assembly of higher-order complexes. Structural studies have indeed demonstrated
 64 the flexibility of ParB molecules, the ability to bridge different *parS* sequences, as well as various
 65 cross-monomer interactions [115,116,122,133]. Notably, the majority of mutational analyses show that
 66 the conserved arginine patch residues are required for ParB spreading and DNA partition, thereby
 67 indicating the crucial role of this motif in ParB functions [68,114,127].

68 Mechanistic insight into the loading of *B. subtilis* Spo0J on *parS* and the role of the conserved
 69 arginine patch was recently provided [122]. Spo0J was shown to hydrolyze cytidine triphosphate
 70 (CTP) with the catalytic center encompassing the arginine patch **GERRFRA** (nucleotide binding
 71 residues in bold). In the presence of *parS*, an open form of the CTP-bound Spo0J dimer favors
 72 cooperative CTP binding and closes into a ring-shaped ParB clamp on *parS* (Figure 2c). The steric
 73 hindrance between *parS* bound HTH motifs was suggested to promote the detachment of the ParB
 74 dimers in a closed conformation from *parS*, as well as sliding away (spreading). CTP hydrolysis is
 75 not required for loading but might instead assist ParB recycling and control ParB spreading, as shown
 76 *in vitro* for *C. crescentus* ParB [140]. Spreading may also be restricted by road blocks formed by NAPs
 77 [122,140]. The role of CTP binding and hydrolysis in ParB-driven partition complex formation was
 78 also shown for *M. xanthus* ParB [141]. Interestingly, in a recent study, Jalal and co-workers
 79 demonstrated that ParBs from various bacterial species show variation in their intrinsic capabilities
 80 for spreading and that the determinant of this variability maps to the N-terminal domain (NTD) [133].
 81 The study used ChIP-seq to analyze ParB spreading in a heterologous host, so the results may not
 82 recapitulate all the determinants affecting the extent of spreading in its original host (like DNA
 83 supercoiling, involvement of other proteins). Nevertheless, this demonstrates that the NTD domain
 84 might evolve to regulate ParB’s association with DNA.

854. ParB Binding to Half-*parS*: A Novel Aspect of ParB–DNA Interactions?

86 A recent ChIP-seq analysis of ParB binding in *P. aeruginosa* added a new dimension to ParB–
87 chromosome interactions [90]. In addition to the ParB-enrichment at *parS*s [64,91] hundreds of
88 additional sites containing a half-*parS* motif (mainly GTTCCAC or GTTTCAC) were also shown to
89 be occupied by *P. aeruginosa* ParB [90]. While ParB binding to four *parS*s proximal to *oriC* resulted in
90 a 50 kbp peak, the width of the ParB peaks around the half-*parS* sites did not exceed 0.6 kbp, even
91 under an abundance of ParB, suggesting a distinct mode of interactions.

92 Interestingly, our analysis of available ChIP-seq data (including the 17 chromosomal ParBs from
93 various species produced in *E. coli* [142] and tested for DNA binding in this heterologous host, as
94 well as two ParBs from *V. cholerae* and *Corynebacterium glutamicum* tested in their native hosts) showed
95 that binding to *parS* half-sites GTTCCAC and GTTTCAC is not a unique feature of *P. aeruginosa* ParB
96 (Figure 3a,b). ParB of *P. aeruginosa* and five other ParBs clearly bind to these heptanucleotides even
97 in a heterologous host. Four ParBs show slightly weaker binding, whereas among the remaining nine
98 including *B. subtilis*, *S. coelicolor*, *V. cholerae*, and *C. glutamicum*, no binding to the selected motifs can
99 be observed. It is feasible that the presence of hundreds of specific ParB–DNA binding sites in the
100 genome enables an additional role of this protein in the modulation of chromosome topology,
101 possibly through the interactions of ParB bound to the half-*parS* with the ParB complex assembled at
102 *parS*s, or through bridging distant DNA segments (Figure 3c). These interactions may play a role in
103 local or global DNA condensation in a species-dependent manner.

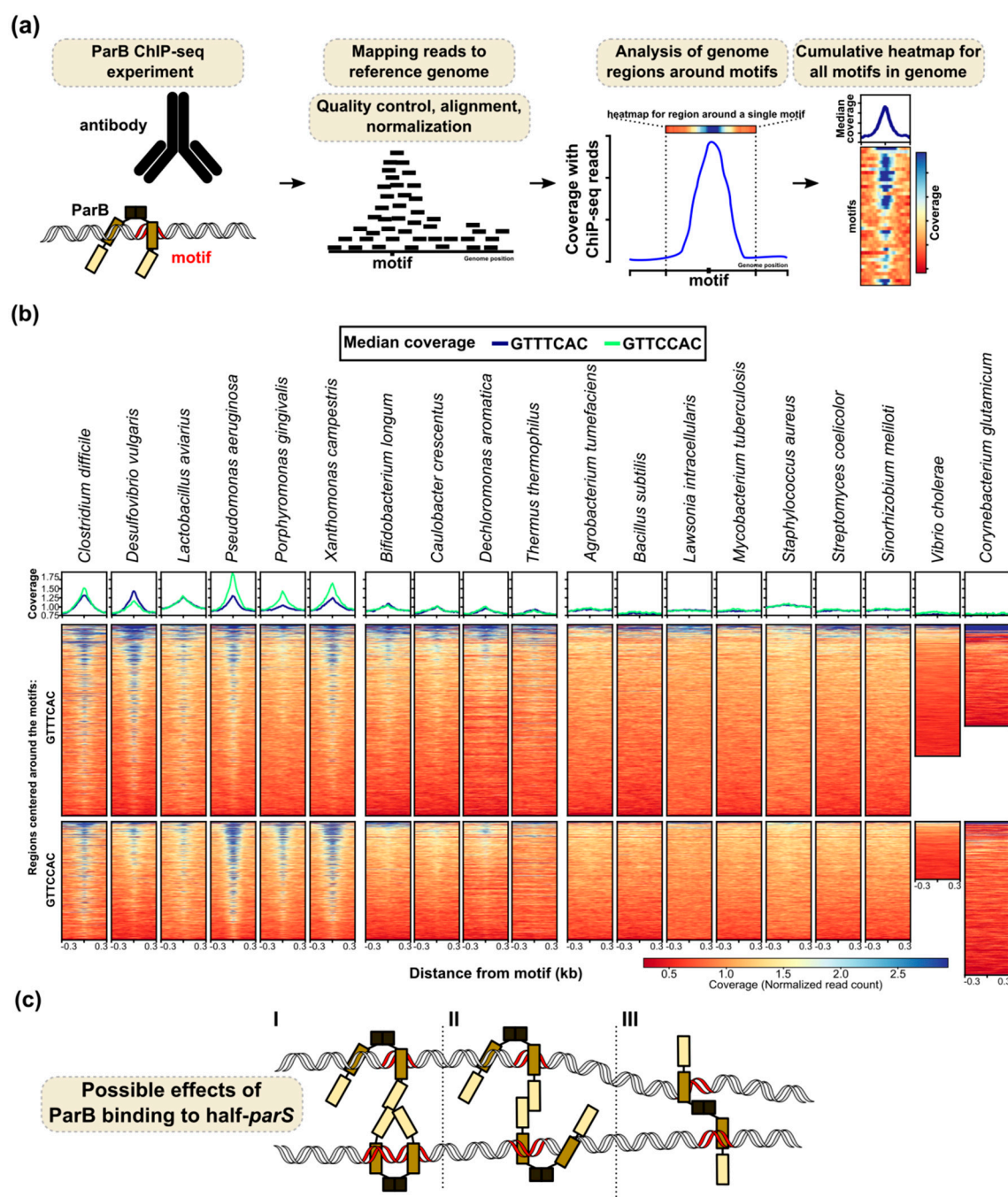


Figure 3. Interactions of ParBs with half-*parS* sites. (a) Outline of the analysis of ParB binding to half-*parS* using the available ParB ChIP-seq data. (b) The binding of ParB proteins from various bacterial species to half-*parS*s assessed by the enrichment of half-*parS* (GTTCCAC and GTTTCAC) containing genomic DNA fragments in the ChIP samples. Heatmaps represent the read coverage for the ParB ChIP samples, calculated for each nucleotide of a ± 300 bp region around all the indicated motifs in the corresponding reference genomes. Plots represent median coverage. A central increase of the coverage indicates enrichment of the DNA containing motif during chromatin immunoprecipitation for the corresponding ParB protein; hence, ParB binds to these sequences. The ChIP-seq data for 17 ParBs from different species produced in *E. coli* [Gene Expression Omnibus GSE129285 [142]], *V. cholerae* ParB1 [GSM3161909, GSM3161911 [129]], and *C. glutamicum* ParB [SRX5581454, SRX5581458, SRX5581460 [72]] were included in the analysis. Raw data were downloaded from the sequence read archive (SRA) and quality-controlled using fastp [143]. Reads were mapped to the reference genomes of *E. coli* K-12 substr. MG1655 (U00096.3), *V. cholerae* O1 biovar El Tor str. N16961 (only chrI, NC_002505.1), and *C. glutamicum* ATCC 13032 (BX927147), respectively, using Bowtie [144] with the $--sensitive$ -local option. Samtools was used to exclude duplicate reads and sort the .bam files [145].

Coverage (.bigwig) files were generated with bamCoverage [146], using the --normalizeUsing RPGC option, without binning and smoothing. Half-*parS* motifs (GTTCCAC and GTTTCAC) were identified in the corresponding genomes using fuzznuc (Emboss 6.6.0). Heatmap displaying coverage with reads in the ParB ChIP data around the identified motifs were generated using plotHeatmap from deepTools [146]. Each line in the heatmap represents the normalized read counts for each nucleotide of a ± 300 bp region around one motif, sorted in the descending order of the mean coverage value and colored according to scale. The median coverage score for the two sets of motifs is presented on plots above the heatmap. For *V. cholerae* and *C. glutamicum*, the data from the biological replicates were averaged. (c) Hypothetical model engaging the half-*parS* sites in DNA structuring. I—The ParB complex loaded at *parS* interacts with an “open” dimeric ParB bound to a half-*parS* site. II—Interactions between two ParB dimers bound to separate half-*parS*s. III—Both monomers in a ParB dimer interact with separate half-*parS*s. All scenarios result in the formation of DNA bridges. In this model, we assume that the binding of ParB to half-*parS* involves the HTH in the central domain.

1335. The Role of ParBs in DNA Topology

The architecture of the origin domain plays an important role in the regulation of replication initiation, global chromosome organization, and DNA segregation [5,16]. The conserved feature of the chromosomal ParAB-*parS* systems is the localization of the *par* operons and the vast majority of *parS* sites within the so-called ori domain, defined as 20% of the chromosome around *oriC* [58,59], suggesting a functional relation. Among all studied bacteria with complete ParAB-*parS* systems, ParB homologs perfectly mark and position the *oriC* regions within the cell, and their absence impairs proper *oriC* localization during the cell cycle [68,71,72,76,82,88,92]. The majority of bacterial species utilizing ParAB-*parS* for DNA segregation contain more than one *parS* sequence close to *oriC* (Table 1421). Nevertheless, a single *parS* site in the vicinity of *oriC* is enough to secure the proper positioning of *oriC* in the cell and segregation of the duplicated *oriC* regions to opposite halves of the cell [80,89,91]. Given the bridging ability of ParB, it is feasible that ParB–ParB interactions may gather the *parS* sites into a single complex. However, microscopy analysis of *C. glutamicum* showed that ParB complexed with distinct *parS* sites could be observed as individual subclusters [72]. The presence of a multiple *parS*s adjacent to *oriC* may therefore secure the proper functioning of segregation machinery and improve its robustness.

In *B. subtilis*, *C. crescentus*, *C. glutamicum*, and *S. pneumoniae*, the nucleoprotein ParB-*parS* complexes around *oriC* serve as platforms recruiting SMC–ScpAB condensin complexes and promoting DNA condensation [5,6,71,147–149]. Two SMC subunits interact with the kleisin ScpA associated with the dimer of the accessory protein ScpB [150–152]. Interactions of ParB-*parS* complexes with SMC complexes direct their binding to DNA in the proximity of *oriC* [5,6,148,152]. Loaded SMC condensin translocates to other parts of the chromosome based on dynamic ATP-dependent transitions between ring-like or open structures [149] and compacts DNA via the loop extrusion mechanism [151,153]. Tethering the two arms of the chromosome together in an ori-ter pattern according to global chromosome organization is dependent on SMC–ScpAB interactions with ParB-*parS* [28,72,148,149,154].

Among bacteria, two other classes of SMC complexes (MukBEF and MksBEF) have also been described. In *E. coli*, MukBEF is required for chromosome segregation but does not facilitate inter-arm contacts, only the long-range co-alignment of chromosomal regions belonging to the same replichores [24,154,155]. No specific loading factor for MukBEF has been identified, suggesting the random loading of condensin complexes on the DNA. In some organisms, such as *P. aeruginosa* or *C. glutamicum*, SMC–ScpAB and MksBEF systems co-exist [72,156,157]. Recent study indicated that in *C. glutamicum*, MksBEFG, in contrast to SMC complex, does not contribute to chromosomal DNA-folding or long-range chromosome interactions but instead it seems to be involved in replication control of low-copy number plasmids [72]. In *M. smegmatis* the maintenance of low-copy number plasmids was enhanced by deletion of the *eptC* gene encoding MukB homologue, suggesting important role of EptC in topology of extrachromosomal elements [157].

S. coelicolor, a representative of Actinobacteria, undergoes drastic changes in chromosome compaction over its complex life cycle. During vegetative growth, elongated hyphal cells are

172 produced with multiple copies of linear uncondensed chromosomes [158]. In sporulating aerial
173 hyphae, unigenomic spores with highly compacted chromosomes are formed. DNA condensation
174 depends on the action of SMC and NAPs specific to sporulation. No indication of ParB–ori complexes
175 recruiting SMC has been reported. Guided by ParA, ParB-bound ori domains were regularly
176 distributed in aerial hyphae before septation in an *smc* mutant but not in the *topA* mutant encoding
177 the single topoisomerase I (TopA) in *S. coelicolor* [158]. Topoisomerases are involved in chromosome
178 topology by maintaining adequate DNA supercoiling, for example, to remove the topological
179 tensions arising during transcription, recombination, and chromosome replication [159]. In linear
180 chromosome of *S. coelicolor*, one of TopA's functions is related to chromosome segregation during
181 sporulation. The depletion of TopA inhibits the efficient separation of paired ParB complexes, which
182 blocks sporulation and retards growth. Sporulation could be at least partially restored by the deletion
183 of *parB*. The direct interactions between ParB–*parS* complexes and TopA suggest that ParB recruits
184 TopA to resolve topological constraints created by ParB interactions with ori domains in *S. coelicolor*
185 [158].

1866. The Role of ParB in the Regulation of Chromosome Replication Initiation

187 ParB of *B. subtilis* was designated Spo0J, and its partner ParA was designated Soj (Suppressor of
188 *spo0J* gene), since the first detected phenotype of strain lacking *spo0J* was a sporulation block, whereas
189 the deletion of both genes restored the process [69]. The role of Spo0J in sporulation results from its
190 indirect involvement in the modulation of DnaA transcriptional regulator activity and its replication
191 initiator activity [160] (Table 2). The latter effect is mediated by Soj, which was shown to act as the
192 negative and positive regulator of DnaA, depending on its nucleotide-bound state [161]. Spo0J
193 stimulates ATP hydrolysis by Soj, as well as the dissociation of Soj dimers. Monomeric Soj interacts
194 with DnaA, disturbing its oligomerization, which is indispensable for replication initiation [162].

195 In the multipartite genomes of *Deinococcus radiodurans* and *V. cholerae* [95,163] the *parB* deletion
196 leads to an increase of the copy number of the cognate replicon. Unlike *B. subtilis*, where Spo0J
197 negatively controls DNA replication through modulation of Soj activity, in these bacteria, direct
198 interactions between ParB and DnaA proteins were detected. *D. radiodurans* ParB1, ParB2, ParB3,
199 encoded by chromosome I, chromosome II, and the megaplasmid, respectively, interact with DnaA
200 and DnaB encoded on chromosome 1 [163]. In the case of *V. cholerae*, both ParA1 and ParB1 directly
201 interact with the DnaA protein [95]. The molecular mechanisms and significance of these interactions
202 remain unclear.

203

Table 2. Interactions of ParBs (or ParB–*parS* complexes) with protein partners and the methods used for their analysis.

Species	ParBs (or ParB– <i>parS</i> complexes) Protein Partners			
	ParA dependent re-locations of ParB– <i>parS</i> complexes	Chromosome <i>ori</i> domain modelling	Localization/anchoring Cell division control	Replication initiation regulation
<i>Bacillus subtilis</i>	+ [70]	SMC; Interplay between SMC and ParB– <i>parS</i> complexes shown by ChIP-seq, FM, and mutational analysis (deletion of <i>parB</i> or <i>parS</i> sites affect SMC foci formation) [5,6]	DivIVA ; Direct interaction confirmed by Co-IP, Spo0J may participate in switching between vegetative growth and sporulation [164]	#DnaA ; Spo0J induces NTPase activity of Soj (ParA), the DnaA regulator [160,161]
<i>Myxococcus xanthus</i>	ND		#PadC ; PadC mediates the binding of ParA to BacNOP cytoskeletal proteins (BLI); ParB may interact with BacNOP through a yet unidentified protein (pull-down) [141,165]	
<i>Mycobacterium smegmatis</i>	+ [166]	SMC; Interplay between SMC and ParB– <i>parS</i> complexes shown by FM and mutational analysis (deletion of <i>parB</i> affects SMC foci formation) [75]	#DivIVA (Wag31) ; ParA interacts with DivIVA and mediates nucleoid anchoring at the cell poles, co-localisation confirmed by the FM of labelled proteins, interactions proven by BACTH and pull-down [166,167]	
<i>Streptococcus pneumoniae</i>	lack of ParA; CpsD , Walker-type ATPase, is involved in ParB– <i>parS</i> movements [168]	SMC; Interplay between SMC and ParB– <i>parS</i> complexes shown by FM and mutational analysis (deletion of <i>parB</i> affects SMC foci formation) [71]	DivIVA ; Direct interactions confirmed by Co-IP and BACTH [169] RocS ; Co-localisation confirmed by FM of labelled proteins, direct interactions confirmed by Co-IP and MST [170], RocS and ParB participate in DNA segregation; CpsD* ; Co-localisation confirmed by FM of fusion proteins, direct interaction (CpsD phosphorylation dependent) confirmed by Co-IP and MST, CpsD and ParB cooperate in coordination with DNA segregation, cell division, and capsule formation [168]	

<i>Streptomyces coelicolor</i>	+	TopA ; Interactions with ParB– <i>parS</i> complexes proven by pull-down, Co-IP, ChIP-seq; these interactions may support chromosome resolution [158]	#ParJ ; ParJ negatively regulates the ParA polymerization indispensable for chromosome segregation, direct interaction confirmed by BACTH and SPR [172] #Scy ; The polarity determinant interacts with ParA, co-localisation confirmed by FM of labelled proteins, direct interactions confirmed by BACTH, co-purification and SPR, ParA and Scy coordinate growth and chromosome segregation [173]
<i>Caulobacter crescentus</i>	+	SMC ; Interplay with ParB– <i>parS</i> complexes shown by Hi-C, ChIP-seq, and mutational analysis, ParB dependent loading also detected on differently positioned <i>parS</i> sites [151]	PopZ* ; Co-localisation confirmed by the FM of labelled proteins, direct interactions confirmed by Co-IP and SPR, EMSA (PopZ with ParB– <i>parS</i> complexes), PopZ–ParB– <i>parS</i> complexes mediate chromosome anchoring to the cell poles [175] #PopZ* ; PopZ interacts also with ParA, co-localisation confirmed by FM of labelled proteins, direct interaction confirmed by Co-IP and SPR, interactions between PopZ and ParA mediate chromosome movement towards the swarmer pole [176] MipZ* ; Co-localisation confirmed by the FM of labelled proteins, direct interactions confirmed by SPR and EMSA (MipZ with ParB– <i>parS</i> complexes), ParB–MipZ complexes control Z-ring positioning [177] #TipN ; The polarity determinant interacts with ParA, direct interactions proven by FM and SPR, ParA–TipN complexes anchor ParB– <i>parS</i> (<i>ori</i> domain) to the new cell pole [103,178]
<i>Corynebacterium glutamicum</i>	+	SMC ; Interplay with ParB– <i>parS</i> complexes shown by FM, ChIP-seq, deletion of <i>parB</i> or <i>parSs</i> results in the loss of SMC loading and foci formation [72]	FtsZ ; Direct interactions confirmed by BACTH [73] PldP* ; Direct interactions confirmed by BACTH [73], putative new cell division control system

<i>Deinococcus radiodurans</i>	+	MinC ; Interactions with ParB1 (chrI), ParB3 (megaplasmid), and ParB4 (plasmid) confirmed by BACTH [180]; DivIVA ; Interactions with ParB1, ParB2, ParB3, and ParB4 confirmed by BACTH and Co-IP [181]; ParB1 interacting with DivIVA may mediate chromosome anchoring to the cell poles and through interactions with FtsZ inhibitor MinC may affect the cell division. Interactions of DivIVA and MinC with ParB2-4 coordinate the segregation of multipartite genome and cell division.	DnaA, DnaB ; interactions with ParB1(chrI) ParB2 (chrII) and ParB3 (megaplasmid), confirmed by BACTH and Co-IP; these interactions probably regulate DNA replication initiation [163]
<i>Vibrio cholerae</i>	+	#HubP ; ParA1 interacts with HubP to mediate nucleoid anchoring at the cell poles; interactions confirmed by the FM of fusion proteins and BACTH [182]	DnaA ; Interactions with ParB1 confirmed by BACTH, a proposed role in the regulation of replication initiation [95]
<i>Hyphomonas neptunium</i>	+	PopZ* ; Co-localisation with ParB– <i>parS</i> in the swarmer cells and in the bud compartments confirmed by the FM of tagged proteins [83]	
<i>Rhodobacter sphaeroides</i>	ND	MipZ* ; Co-localization demonstrated by the FM of fusion proteins; direct interactions confirmed by BACTH; the ParB–MipZ system supports the Z-ring assembly and its stability [183]	
<i>Magnetospirillum gryphiswaldense</i>	ND	MipZ1* ; Co-localization demonstrated by the FM of fusion proteins; direct interactions confirmed by BLI, ParB–MipZ1 system controls Z-ring positioning; MipZ2* may also interact with ParB [184]	

204 ND: not determined; #: Indirect interactions mediated by the cognate ParAs; *:ParA-like protein, Walker-type ATPase; **FM**: Fluorescence
 205 microscopy; **BACTH**: Bacterial two hybrid system; **Co-IP**: Co-immunoprecipitation; **Hi-C**: chromosome conformation capture; **ChIP-seq**:
 206 Chromatin immunoprecipitation followed by DNA sequencing; **SPR**: Surface plasmon resonance; **EMSA**: Electrophoretic mobility shift assay; **MST**:
 207 Microscale thermophoresis; **BLI**: Bio-layer interferometry.

2087. Involvement of ParB in The Nucleoid Occlusion

209 Deletion of the *spo0J* gene from the *B. subtilis* chromosome results not only in aberrant DNA
210 replication and sporulation but also affects cell division [70]. Elongated cells were detected in
211 populations of strains deprived of Spo0J or both, Spo0J and Soj, but not in the strain lacking only Soj
212 [70]. In *B. subtilis*, two systems controlling cell division were described (for a review, see [185]). The
213 Min system hampers the formation of the cytokinetic Z-ring composed of tubulin like FtsZ protein
214 close to the cell poles [186]. The nucleoid occlusion (NO) system prevents premature Z-ring formation
215 over the nucleoid until most of the chromosomal DNA has been segregated. Spo0J together with its
216 paralog, Noc [187–189], block premature Z-ring assembly, preventing chromosome guillotining in
217 the dividing cells. The deletion of either *noc* (initially named *yjaA*) or *spo0J* results in aberrant cell
218 division, and the deletion of both *noc* and *spo0J* has a synergistic effect, potentiating the aberrations
219 [190].

2208. The Interactions of ParB with Topological Determinants during Cell Division

221 Another aspect of ParB's involvement in the cell division process is its interplay with proteins
222 located at the cell poles, such as DivIVA in *B. subtilis* [164] (Table 2). DivIVA is a highly conserved
223 component of the Min system (equivalent to the *E. coli* MinE protein in the MinCDE system) in a wide
224 range of Gram-positive bacteria (for a review, see [191]). The biological functions and significance of
225 DivIVA vary among different bacterial species. However, the primary role of DivIVA (as one of the
226 Min proteins) seems to be the proper positioning of the cell division site. Since Spo0J–DivIVA
227 interactions are observed in *B. subtilis* only during the early stages of sporulation when DivIVA
228 supports Spo0J-*parS* guided orientation of the chromosome and its polar attachment, it is postulated
229 that DivIVA is also involved in the molecular switch between vegetative cell division and spore
230 formation [164].

231 Interactions between DivIVA and ParB were also detected in the non-sporulating bacteria *S.*
232 *pneumoniae* [169] and *D. radiodurans* [180,181]. In the latter, DivIVA interacts with various ParBs
233 encoded by the multipartite genome, with ParB1 (chrI), ParB2 (chrII), and ParB3 and ParB4 from the
234 megaplasmid and plasmid, respectively. In the case of *D. radiodurans*, ParB1, ParB3, and ParB4 also
235 interact with another Min protein—MinC that functions as an FtsZ polymerization inhibitor [180].

236 It should be noted that, in some cases, ParB may be indirectly engaged in ori domain anchoring
237 (Table 2). In *Mycobacterium smegmatis*, ParA, instead of ParB, interacts directly with DivIVA [166]. In
238 *S. coelicolor*, both ParA and ParB are involved in localization of the segrosome in hyphae [171].
239 However, only ParA interacts with so-called 'polarisome' or tip-organizing complex (TIPOC), which
240 includes DivIVA and the coiled-coil protein, Scy, and anchors the segrosome at the tips. Whereas
241 ParA and Scy direct interactions have been confirmed [173], there is no evidence for ParA (or ParB)
242 and DivIVA interactions in *S. coelicolor* [191]. In *C. crescentus*, ParA mediates the ParB–DNA
243 complex's positioning at the new cell pole via interactions with the TipN protein [178]. In *V. cholerae*,
244 ParB1-*oriC1* complex is targeted to the cell pole via interactions between the polar protein HubP and
245 ParA1 [182].

246 In α -proteobacteria, lacking Min and NO systems, ParB interacts with PopZ, polar organizing
247 protein Z (DivIVA functional equivalent), and MipZ, the mid-cell positioning of the FtsZ protein
248 [175,177,192]. PopZ is a key component in the regulation and coordination of chromosome replication
249 and partitioning in *C. crescentus*, a bacterium with a dimorphic lifestyle (for a review, see [193]). In
250 this organism, cell division leads to the formation of a mobile swarmer cell and a non-mobile stalker
251 cell. However, only the latter is able to duplicate [194]. The ori domain of the longitudinally oriented
252 chromosome is anchored to the stalked pole by direct interactions between ParB-*parS* and PopZ [175].
253 Immediately after DNA replication initiation, one of the duplicated ori domains begins translocation
254 towards the opposite pole, assisted by the ParAB-*parS* system. Simultaneously, the mono-polar
255 localization of PopZ is switched to the bi-polar localization, and the transferred ParB-*parS* complex
256 (ori domain) is attached to the cell membrane via the PopZ protein complex at the swarmer pole
257 [192]. At this stage of the chromosome segregation also ParA directly interacts with PopZ protein
258 [176].

In the marine alpha-proteobacterium, *Hyphomonas neptunium*, which proliferates by bud formation at the tip of a stalk-like cellular compartment, a unique two-step chromosome segregation process occurs [83]. Initially, two newly replicated ori domains are segregated to opposite poles of the mother cell via a ParAB-*parS* dependent mechanism. When the bulk of the chromosome has been replicated, the cell produces a bud (swarmer cell), and a next segregation step largely independent of replication begins. This step involves the translocation of a stalk-proximal ParB-origin region through the stalk to the bud compartment by an unknown mechanism. PopZ's homolog from *H. neptunium* associates with the ParB-*parS* complex in swarmer cells and in the bud compartment at a later stage of the cell cycle, possibly acting as a tether for the ori domain at the new bud pole [83].

DNA segregation and the PopZ mediated attachment of ParB-*parS* complexes at the cell poles are critical for the appropriate positioning and formation of the cytokinetic Z-ring. In *C. crescentus*, ParB is also involved in the formation of a bi-polar gradient of MipZ, a polymerization inhibitor of the FtsZ protein, and both ParB and MipZ are indispensable [177]. ParB stimulates the formation of MipZ dimers, negatively affecting the polymerization of FtsZ and hence Z-ring formation [177]. MipZ dimers are also able to bind DNA in a non-specific manner [195]. This binding stimulates MipZ ATPase activity and promotes dimer dissociation, which results in a release of MipZ monomers from the DNA [196]. In *C. crescentus*, MipZ forms a bipolar comet-like gradient with the highest concentration of MipZ in the cell poles and the lowest concentration in the midcell before division. This distribution of MipZ depends on the ParB-*parS* complex movement from the stalked pole to the swarmer pole and promotes Z-ring positioning at the midcell. In another representative of α -proteobacteria, *Rhodobacter sphaeroides*, the bipolar comet-like gradient of MipZ was not detected [183]. Detailed studies revealed that *R. sphaeroides* MipZ, similarly to *C. crescentus* MipZ, interacts with ParB as a monomer and inhibits FtsZ as a dimer. However, in this organism, MipZ dimers are never present at the cell poles but form a ring-like structure at the midcell, facilitating Z-ring assembly and stability rather than Z-ring positioning (as was postulated for *C. crescentus*) [183].

Finally, a functional analysis of two MipZ-like proteins encoded by *mipZ1* and *mipZ2* in *Magnetospirillum gryphiswaldense* revealed that MipZ1 is crucial for proper cell division, and MipZ2 has only a minor effect on this process [184]. MipZ1 interacts with ParB and forms a bipolar comet-like gradient akin to MipZ of *C. crescentus*, while MipZ2 localizes to the cell division site similar to the MipZ of *R. sphaeroides* [184].

The role of ParB in cell division was also postulated in *C. glutamicum* [73]. Similarly to *C. crescentus*, *C. glutamicum* lacks Min and NO systems. *C. glutamicum* ParB interacts not only with ParA but also with the ParA homologue, the PldP protein (with a 62% sequence similarity). Analysis of the *pldP* mutant showed significant defects in the cell division, comparable to *E. coli* and *B. subtilis* mutants in *min* genes [73]. *In vitro*, ParB interacts not only with PldP but also with the FtsZ protein. It is not clear at which stage of the cell cycle the crosstalk between DNA segregation and cell division takes place. A fluorescently labelled PldP protein can be detected as visible foci near the cell division site, but diffused PldP is also present in the cytoplasm [73].

2979. ParB's Role in Capsule Formation in *S. pneumoniae*

In *S. pneumoniae*, ParB interacts with DivIVA during cell division. It has also been shown that ParB participates in specific crosstalk between DNA segregation, cell division, and capsule formation in this organism [168,170]. *S. pneumoniae*'s incomplete Par(A)B-*parS* system consists of four *parS* sites close to *oriC*, as well as an orphan *parB* gene [197]. The deletion of *parB* impairs chromosome segregation but only in a minor way and has no influence on bacterial growth [71]. Recent reports have shed light on the role of *S. pneumoniae* ParB, showing that it cooperates with two proteins, CpsD and RocS [168,170]. Capsular polysaccharide protein D (CpsD), a ParA-like ATPase, is a component of a protein complex involved in the synthesis and export of capsular polysaccharide. Together with the membrane associated CpsC, it forms a tyrosine autokinase. Autophosphorylated CpsD stimulates ParB-*parS* binding and promotes chromosome segregation, as well as cell division and capsule formation. Non phosphorylated CpsD delays ParB-*parS* translocation to the cell equator and negatively affects cell division [168]. Another ParB partner, RocS (Regulator of chromosome

Segregation), was initially identified as a CpsD partner in the control of cell division [170]. RocS is a non-specific DNA binding protein, with a N-terminal MarR-like HTH motif and a C-terminal MinD-like cell membrane binding helix [170]. RocS and ParB seem to have partially overlapping functions in *S. pneumoniae*, and a double deletion of *rocS* and *parB* is lethal. However, the lack of RocS has a more deleterious effect on DNA segregation than ParB deficiency alone [170]. In contrast to ParB, RocS is not involved in capsule formation but is directly involved in cell division control through CpsD. Thus, in *S. pneumoniae*, this unique system, involving ParB, RocS, and CpsD (CpsC) proteins, coordinates and secures DNA segregation, cell division, but also capsule formation, which is critical for bacterial virulence [170].

10. Impact of ParBs on Gene Expression

The autoregulation of partition operon expression is a common feature of plasmidic systems [41]. However, in the Class Ia type of *par* loci, ParA acts as a repressor, binding in the promoter region of the *parAB* operon, whereas ParB usually works as a co-repressor [41,99,100]. The known examples of plasmidic ParBs of Class Ia playing the role of the global transcriptional regulators include the KorBs of IncP-1 plasmids [126,198,199] and related KorB of IncU plasmids [200].

For chromosomal ParB proteins, artificial insertion of the *parS* sequence upstream of the *repA* promoter in the test plasmid was used to demonstrate the negative effect of *P. aeruginosa* ParB binding to *parS* on expression of the adjacent genes [64]. The flexibility of ParBs in self-interactions via the use of NTDs and CTDs, specific and unspecific interactions with DNA and interactions with multiple partners (Figure 4) may facilitate the formation of the expanded ParBs network, potentially influencing gene expression.

In recent years, the relation between ParB binding to chromosomal DNA and the expression of loci close to the corresponding *parS* sites has been systematically investigated using a combination of ChIP methods and genome-wide transcriptomic approaches. In *B. subtilis*, Spo0J was observed to bind to and around 10 *parS* sequences. However, a lack of Spo0J did not affect the expression of genes adjacent to these sites [68]. Spo0J deficiency resulted in an elevated expression of only the *fruR* gene (encoding a putative transcriptional regulator), whereas the mRNA levels of nine other genes, among them, the sporulation genes *spoIIIGA*, *cotE*, *cotG*, *spoIIAA*, and *sigE*, were decreased [68]. This negative effect of sporulation gene regulation can be explained by the influence of Spo0J deficiency on the Soj mediated activation of the Sda replication check point [160].

The influence of ParB on gene expression was also studied in *V. cholerae*, a bacterium with two chromosomes, each encoding their own partitioning system (*parABS1* and *parABS2*). Chromatin precipitation combined with the microarray technique (ChIP-chip) confirmed that ParB1 bound to three *parS* motifs and spread for 16 kbp [132]. The transcriptomic analysis of the Δ *parB1* mutant revealed a changed expression of only three genes in the region occupied by ParB and several more outside of this region. Cloning promoters of these three genes upstream of the promoter-less *lacZ* on the plasmid eliminated the regulatory effect of ParB1, indicating that genetic localization and/or DNA topology play a role in the regulation of these promoters by ParB1. The role of ParB1 in controlling gene expression outside of the highly ParB-enriched zone was postulated to be indirect through interactions with other regulatory proteins [132].

A similar transcriptional analysis in *S. pneumoniae* showed that a lack of ParB affected the expression of eight genes. However, none of these genes were located in proximity to the four *parS* sequences identified in this organism [130]. Significantly, ParB deficiency resulted in a modest increase in the expression of the *comCDE* operon involved in the regulation of competence and located 5 kbp away from *parS* (−1.6°) [130]. Mutating *parS* (−1.6°) to block ParB binding was sufficient to induce *comCDE* expression, suggesting that a ParB complex formed at a single *parS* may influence the expression of promoters at a distance. Attempts to recapitulate this effect with the insertion of a strong synthetic promoter in the region failed, suggesting a highly selective mechanism by which the ParB complex at *parS* (−1.6°) influences *comCDE* expression and, as a result, the development of the competence cascade [130].

The genome wide transcriptome analyses presented above indicate that ParB deficiency results in minor changes in the cell transcriptomes of the tested species. However, the analysis of ParB deficient *P. aeruginosa* cells from exponentially growing cultures in rich medium showed expression changes for 1166 genes, which is around 20% of all loci [201]. Additionally, global changes in the transcriptome were also observed in ParA deficient cells; 697 genes showed altered expression in the $\Delta parA$ mutant, and 77% of them overlapped with the gene pool affected by ParB deficiency [201]. This overlap is not surprising, as previous data indicated that ParA deficiency in this organism promotes ParB degradation [92]. The wide range of changes in the transcriptomes of *par* mutants reflect a wide spectrum of various growth defects. The lack of *parA* or *parB* in *P. aeruginosa* leads up to a 1000-fold increase in the number of cells with defects in their chromosome segregation, extended division times, longer cells, altered colony morphology, and impaired swimming and swarming motility [92,202]. We cannot exclude that observed changes in the expression of some genes result from the aberrations in ParB and/or ParA dependent processes like DNA segregation although anucleate cells constitute only 2%–4% of population under analyzed conditions. Significantly, not only depletion, but also mild overproduction of ParB protein lead to global transcriptome changes in *P. aeruginosa* [203].

P. aeruginosa ParB binds to a cluster of four *parS* sequences (*parS1-4*) in the vicinity of *oriC* to form a large nucleoprotein complex, and the binding to one of these sites is required and sufficient for proper chromosome segregation [89–91]. The analysis of the mRNA levels of genes adjacent to *parS1-4* showed that direct ParB interactions with intergenic *parS3* and *parS4* motifs located upstream of *PA0011* and *PA0013*, respectively, repressed their expression, while the expression of other genes in the analysed region was unchanged in the *parB* and *parS1-4* deficient cells [203]. Concomitantly, a mild overproduction of ParB led to a more pronounced transcriptional silencing of the majority of genes in the vicinity of the *parS1-4* cluster. This observation suggests that the size, composition, or stability of the ParB nucleoprotein complex may dictate the effect on gene expression [203]. Strikingly, our recent study demonstrated that in *P. aeruginosa*, ParB was bound to numerous sites containing a heptanucleotide half-*parS*. However, the binding to half-*parS* sites may not directly account for the transcriptome changes ParB exerts. Only 15% of ParB enriched half-*parS* sites localizes in intergenic regions with putative transcriptional initiation signals [90]. Binding of *P. aeruginosa* ParB to hundreds of specific DNA motifs may have a great impact on chromosome topology (Figure 3c). ParBs from several other bacterial species also bind to GTTCCAC and GTTTCAC sequences (Figure 3b), indicating that *P. aeruginosa* ParB is not unique in this mode of interaction. The significance of these interactions in cell processes (including gene expression regulation) requires further studies.

11. Conclusions and Future Perspectives

ParAB-*parS* systems are encoded close to *oriCs* in the chromosomes of most bacterial species [41,59]. The primary role of ParAB-*parS* systems is undoubtedly the segregation of newly replicated DNA. ParB binding to *parSs* in the proximity of *oriC*, structuring *ori* domains, directing their motion with the help of the ParA partner, and the anchoring of *ori* domains at the defined locations are vital for accurate segregation of the genomes. With a few exceptions (Table 1), this system is not essential for cell survival but rather an accessory to hypothetical but attractively more universal entropy-driven DNA segregation machinery [204,205]. In some species, like *T. thermophilus*, the ParAB-*parS* system seems not to be involved at all in DNA segregation [98]. New sophisticated molecular biology methods revealed the details of chromosome segregation, providing insight into the formation and structure of the ParB nucleoprotein complex, as well as the mechanisms responsible for its relocation to specific cell positions. Nevertheless, the picture of this process is far from complete. The diversity of the Par partners (Table 2 and Figure 4) and the species-specific requirements for cell cycle proceedings still lead to new exciting discoveries [83,206].

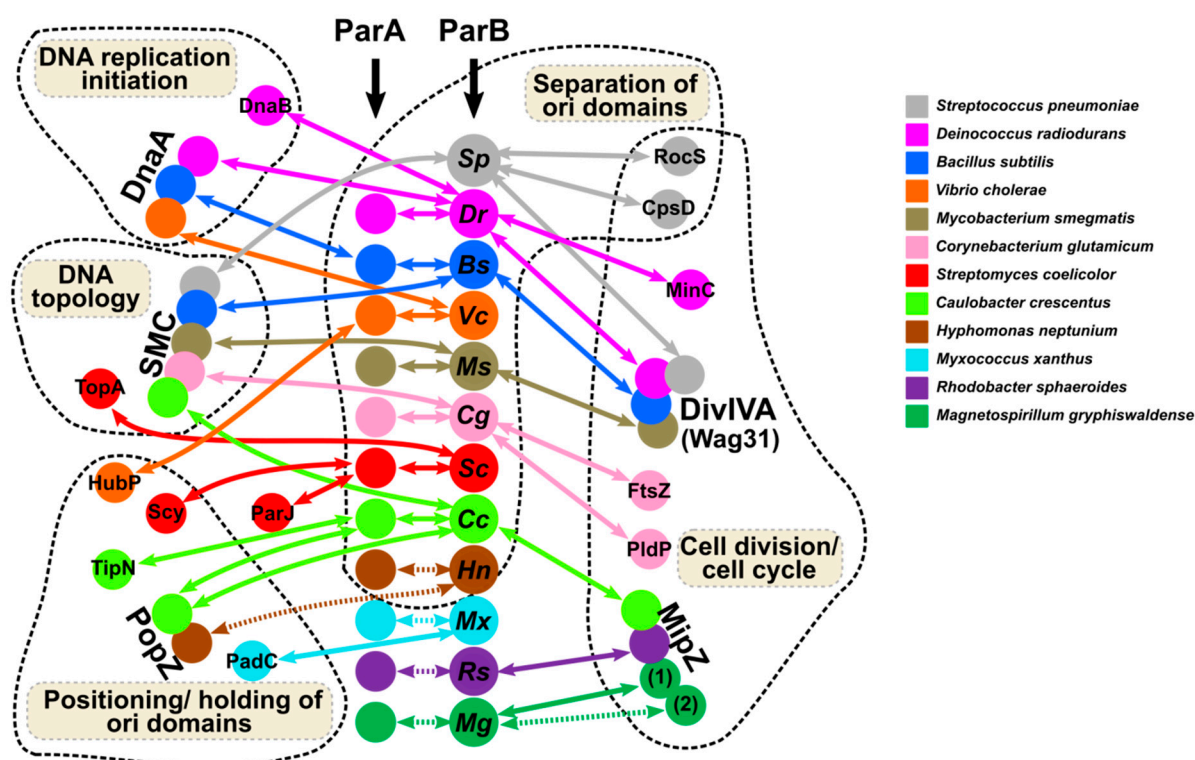


Figure 4. Network of ParBs interactions with ParAs and other partners coordinating chromosome segregation with various cellular functions in the analyzed bacterial species. The dashed arrows indicate interactions not yet confirmed experimentally.

ParB proteins seem to be engaged in crosstalk between DNA segregation, DNA replication, cell growth, and division. The synchrony of these processes in non-compartmentalized cells emphasizes the significance of such crosstalk (reviewed in [193]). The ParBs domain's composition and structural flexibility facilitates various modes of interactions with specific (*parS* and half-*parS* sites) and non-specific DNA and points to multiple interfaces for self-interactions and cooperation with different protein partners. The involvement of ParBs in a variety of cell functions directly through direct interactions with vital cell components or indirectly using their primary partners, ParAs, is summarized in Figure 4. To achieve that, they target similar main players in different species (DnaA, SMC, DivIVA, MipZ) or adapt to species-specific factors playing the same function, such as a polar positioning.

The role of ParB as a transcriptional regulator has been shown in a limited number of species and for a limited number of genes, not necessarily located close to the *parS* sites. The most intriguing is the biological significance of ParB binding to half-*parS*s observed in some species, despite the common occurrence of these motifs in the genomes. In *P. aeruginosa* and a few other species ParB binds to hundreds of half-*parS* sites (Figure 3b). These interactions may induce topological constraints leading to the observed ParB role as a global transcriptional regulator in *P. aeruginosa* [201].

One of the most poorly understood aspects of ParBs functioning is the nature of molecular switches that control the level and activity/conformation of ParBs. Par proteins are not as abundant as histone-like proteins [68,92]. The level of Par proteins, possibly influencing their activities, could be controlled by different mechanisms. The regulation of *parB* and *parA* expression has only been partially studied in a limited number of bacteria species (e.g., [84,132,207,208]). Alternatively, the levels of Par proteins could be modulated by cell proteases, e.g. depending on the phase of growth [92].

The observation that ParB loading at *parS* and sliding on DNA requires CTP binding [122,140,141], a key metabolite in DNA and phospholipids synthesis, adds CTP to the players possibly regulating the ParB–DNA interactions. The motif containing amino acid residues responsible for CTP binding and ParB CTPase activity is one of the most conserved elements within

the ParB protein sequences [122,141]. This suggests that CTP binding and hydrolysis may be crucial for proper ParB functioning, not only in the abovementioned *B. subtilis* [122], *M. xanthus* [141] and *C. crescentus* [133], but also in other bacteria encoding ParAB-*parS* systems.

An increasing number of important bacterial proteins have been shown to undergo post-translational modifications (PTMs), such as phosphorylation or acetylation [209–211]. *M. tuberculosis* ParB is phosphorylated by Serine/Threonine Protein Kinases (STPKs), including PknB, a key component of the signal transduction pathway that regulates, for example, cell division and the survival of the pathogen in the host [212,213]. This PTM negatively affects ParB's DNA binding properties in vitro, as well as ParB interactions with the cognate ParA protein partner. The regulation of ParB activity by direct phosphorylation or acetylation is not the only way to affect its activity, as its partners' activity may be dependent on PTM. For example, the functions of *S. pneumoniae* ParB depend on interactions with the membrane bound CpsC/D tyrosine auto-kinase [168]. We also cannot exclude the possibility that CpsC/D phosphorylates *S. pneumoniae* ParB, like in the case of *M. tuberculosis* auto-kinases from the STPK family [212].

The biological roles of chromosomally encoded ParBs and the molecular basis of their functions are more complex than was previously thought. It is clear that despite the significant conservation of chromosomal ParAB-*parS* systems, these systems evolved independently in different bacterial species. ParBs seem to be excellent models for studying many aspects of bacterial molecular biology and genome evolution.

Funding: This work was financed by the Polish National Science Centre, grant no 2018/29/B/NZ2/01745 awarded to GJB.

Conflicts of Interest: The authors declare no conflict of interest. The funders had no role in the design of the study; in the collection, analyses, or interpretation of data; in the writing of the manuscript, or in the decision to publish the results.

References

1. Dame, R.T.; Rashid, F.-Z.M.; Grainger, D.C. Chromosome organization in bacteria: Mechanistic insights into genome structure and function. *Nat. Rev. Genet.* **2019**, , doi:10.1038/s41576-019-0185-4.
2. Badrinarayanan, A.; Le, T.B.; Laub, M.T. Bacterial chromosome organization and segregation. *Annu. Rev. Cell Dev. Biol.* **2015**, *31*, 171–199.
3. Dorman, C.J. Genome architecture and global gene regulation in bacteria: Making progress towards a unified model? *Nat. Rev. Microbiol.* **2013**, *11*, 349–355.
4. Dame, R.T.; Tark-Dame, M. Bacterial chromatin: Converging views at different scales. *Curr. Opin. Cell Biol.* **2016**, *40*, 60–65.
5. Gruber, S.; Errington, J. Recruitment of condensin to replication origin regions by ParB/Spo0J promotes chromosome segregation in *B. subtilis*. *Cell* **2009**, *137*, 685–696.
6. Sullivan, N.L.; Marquis, K.A.; Rudner, D.Z. Recruitment of SMC by ParB-*parS* organizes the origin region and promotes efficient chromosome segregation. *Cell* **2009**, *137*, 697–707.
7. Schwartz, M.A.; Shapiro, L. An SMC ATPase mutant disrupts chromosome segregation in *Caulobacter*. *Mol. Microbiol.* **2011**, *82*, 1359–1374.
8. Dillon, S.C.; Dorman, C.J. Bacterial nucleoid-associated proteins, nucleoid structure and gene expression. *Nat. Rev. Microbiol.* **2010**, *8*, 185–195.
9. Le, T.B.K.; Imakaev, M.V.; Mirny, L.A.; Laub, M.T. High-resolution mapping of the spatial organization of a bacterial chromosome. *Science* **2013**, *342*, 731–734.
10. Reyes-Lamothe, R.; Sherratt, D.J. The bacterial cell cycle, chromosome inheritance and cell growth. *Nat. Rev. Microbiol.* **2019**, *17*, 467–478.
11. Wang, X.; Montero Llopis, P.; Rudner, D.Z. Organization and segregation of bacterial chromosomes. *Nat. Rev. Genet.* **2013**, *14*, 191–203.
12. Bouet, J.-Y.; Stouf, M.; Lebailly, E.; Cornet, F. Mechanisms for chromosome segregation. *Curr. Opin. Microbiol.* **2014**, *22*, 60–65.
13. Valens, M.; Penaud, S.; Rossignol, M.; Cornet, F.; Boccard, F. Macrodome organization of the *Escherichia coli* chromosome. *EMBO J.* **2004**, *23*, 4330–4341.

48914. Dame, R.T.; Kalmykova, O.J.; Grainger, D.C. Chromosomal macrodomains and associated proteins:
490 Implications for DNA organization and replication in Gram-negative bacteria. *PLoS Genet.* **2011**, *7*,
491 e1002123, doi:10.1371/journal.pgen.1002123.
49215. Surovtsev, I.V.; Jacobs-Wagner, C. Subcellular organization: A critical feature of bacterial cell replication.
493 *Cell* **2018**, *172*, 1271–1293.
49416. Marbouty, M.; Le Gall, A.; Cattoni, D.I.; Cournac, A.; Koh, A.; Fiche, J.-B.; Mozziconacci, J.; Murray, H.;
495 Koszul, R.; Nollmann, M. Condensin- and replication-mediated bacterial chromosome folding and origin
496 condensation revealed by Hi-C and super-resolution imaging. *Mol. Cell* **2015**, *59*, 588–602.
49717. Niki, H.; Yamaichi, Y.; Hiraga, S. Dynamic organization of chromosomal DNA in *Escherichia coli*. *Genes Dev.*
498 **2000**, *14*, 212–223.
49918. Espeli, O.; Mercier, R.; Boccard, F. DNA dynamics vary according to macrodomain topography in the *E.*
500 *coli* chromosome. *Mol. Microbiol.* **2008**, *68*, 1418–1427.
50119. Dorman, C.J. Co-operative roles for DNA supercoiling and nucleoid-associated proteins in the regulation
502 of bacterial transcription. *Biochem. Soc. Trans.* **2013**, *41*, 542–547.
50320. Val, M.-E.; Marbouty, M.; de Lemos Martins, F.; Kennedy, S.P.; Kemble, H.; Bland, M.J.; Possoz, C.; Koszul,
504 R.; Skovgaard, O.; Mazel, D. A checkpoint control orchestrates the replication of the two chromosomes of
505 *Vibrio cholerae*. *Sci. Adv.* **2016**, *2*, e1501914, doi:10.1126/sciadv.1501914.
50621. Higgins, N.P. Species-specific supercoil dynamics of the bacterial nucleoid. *Biophys. Rev.* **2016**, *8*, 113–121.
50722. Le, T.B.; Laub, M.T. Transcription rate and transcript length drive formation of chromosomal interaction
508 domain boundaries. *EMBO J.* **2016**, *35*, 1582–1595.
50923. Browning, D.F.; Grainger, D.C.; Busby, S.J. Effects of nucleoid-associated proteins on bacterial chromosome
510 structure and gene expression. *Curr. Opin. Microbiol.* **2010**, *13*, 773–780.
51124. Lioy, V.S.; Cournac, A.; Marbouty, M.; Duigou, S.; Mozziconacci, J.; Espeli, O.; Boccard, F.; Koszul, R.
512 Multiscale structuring of the *E. coli* chromosome by nucleoid-associated and condensin proteins. *Cell* **2018**,
513 *172*, 771–783.
51425. Danilova, O.; Reyes-Lamothe, R.; Pinskaya, M.; Sherratt, D.; Possoz, C. MukB colocalizes with the *oriC*
515 region and is required for organization of the two *Escherichia coli* chromosome arms into separate cell
516 halves. *Mol. Microbiol.* **2007**, *65*, 1485–1492.
51726. Petrushenko, Z.M.; Cui, Y.; She, W.; Rybenkov, V.V. Mechanics of DNA bridging by bacterial condensin
518 MukBEF *in vitro* and *in singulo*. *EMBO J.* **2010**, *29*, 1126–1135.
51927. Strunnikov, A.V. SMC complexes in bacterial chromosome condensation and segregation. *Plasmid* **2006**, *55*,
520 135–144.
52128. Wang, X.; Le, T.B.K.; Lajoie, B.R.; Dekker, J.; Laub, M.T.; Rudner, D.Z. Condensin promotes the
522 juxtaposition of DNA flanking its loading site in *Bacillus subtilis*. *Genes Dev.* **2015**, *29*, 1661–1675.
52329. Trussart, M.; Yus, E.; Martinez, S.; Baù, D.; Tahara, Y.O.; Pengo, T.; Widjaja, M.; Kretschmer, S.; Swoger, J.;
524 Djordjevic, S.; et al. Defined chromosome structure in the genome-reduced bacterium *Mycoplasma*
525 *pneumoniae*. *Nat. Commun.* **2017**, *8*, 14665.
52630. Vallet-Gely, I.; Boccard, F. Chromosomal organization and segregation in *Pseudomonas aeruginosa*. *PLoS*
527 *Genet.* **2013**, *9*, e1003492, doi:10.1371/journal.pgen.1003492.
52831. Harms, A.; Treuner-Lange, A.; Schumacher, D.; Søgaard-Andersen, L. Tracking of chromosome and
529 replisome dynamics in *Myxococcus xanthus* reveals a novel chromosome arrangement. *PLoS Genet.* **2013**, *9*,
530 e1003802, doi:10.1371/journal.pgen.1003802.
53132. Viollier, P.H.; Thanbichler, M.; McGrath, P.T.; West, L.; Meewan, M.; McAdams, H.H.; Shapiro, L. Rapid
532 and sequential movement of individual chromosomal loci to specific subcellular locations during bacterial
533 DNA replication. *Proc. Natl. Acad. Sci. USA.* **2004**, *101*, 9257–9262.
53433. Umbarger, M.A.; Toro, E.; Wright, M.A.; Porreca, G.J.; Baù, D.; Hong, S.-H.; Fero, M.J.; Zhu, L.J.; Marti-
535 Renom, M.A.; McAdams, H.H.; et al. The three-dimensional architecture of a bacterial genome and its
536 alteration by genetic perturbation. *Mol. Cell* **2011**, *44*, 252–264.
53734. Marbouty, M.; Cournac, A.; Flot, J.-F.; Marie-Nelly, H.; Mozziconacci, J.; Koszul, R. Metagenomic
538 chromosome conformation capture (meta3C) unveils the diversity of chromosome organization in
539 microorganisms. *ELife* **2014**, *3*, e03318, doi:10.7554/eLife.03318.
54035. Nielsen, H.J.; Ottesen, J.R.; Youngren, B.; Austin, S.J.; Hansen, F.G. The *Escherichia coli* chromosome is
541 organized with the left and right chromosome arms in separate cell halves. *Mol. Microbiol.* **2006**, *62*, 331–
542 338.

54336. Wang, X.; Liu, X.; Possoz, C.; Sherratt, D.J. The two *Escherichia coli* chromosome arms locate to separate cell
544 halves. *Genes Dev.* **2006**, *20*, 1727–1731.
54537. Nordström, K.; Molin, S.; Aagaard-Hansen, H. Partitioning of plasmid R1 in *Escherichia coli*: I. Kinetics of
546 loss of plasmid derivatives deleted of the par region. *Plasmid* **1980**, *4*, 215–227.
54738. Austin, S.; Abeles, A. Partition of unit-copy miniplasmids to daughter cells. II. The partition region of
548 miniplasmid P1 encodes an essential protein and a centromere-like site at which it acts. *J. Mol. Biol.* **1983**,
549 *169*, 373–387.
55039. Abeles, A.L.; Friedman, S.A.; Austin, S.J. Partition of unit-copy miniplasmids to daughter cells. III. The
551 DNA sequence and functional organization of the P1 partition region. *J. Mol. Biol.* **1985**, *185*, 261–272.
55240. Gerdes, K.; Larsen, J.E.; Molin, S. Stable inheritance of plasmid R1 requires two different loci. *J. Bacteriol.*
553 **1985**, *161*, 292–298.
55441. Gerdes, K.; Møller-Jensen, J.; Jensen, R.B. Plasmid and chromosome partitioning: Surprises from
555 phylogeny. *Mol. Microbiol.* **2000**, *37*, 455–466.
55642. Gerdes, K.; Howard, M.; Szardenings, F. Pushing and pulling in prokaryotic DNA segregation. *Cell* **2010**,
557 *141*, 927–942.
55843. Hayes, F. The partition system of multidrug resistance plasmid TP228 includes a novel protein that
559 epitomizes an evolutionarily distinct subgroup of the ParA superfamily. *Mol. Microbiol.* **2000**, *37*, 528–541.
56044. Motallebi-Veshareh, M.; Rouch, D.A.; Thomas, C.M. A family of ATPases involved in active partitioning
561 of diverse bacterial plasmids. *Mol. Microbiol.* **1990**, *4*, 1455–1463.
56245. Koonin, E.V. A superfamily of ATPases with diverse functions containing either classical or deviant ATP-
563 binding motif. *J. Mol. Biol.* **1993**, *229*, 1165–1174.
56446. Møller-Jensen, J.; Borch, J.; Dam, M.; Jensen, R.B.; Roepstorff, P.; Gerdes, K. Bacterial mitosis: ParM of
565 plasmid R1 moves plasmid DNA by an actin-like insertional polymerization mechanism. *Mol. Cell* **2003**, *12*,
566 1477–1487.
56747. Larsen, R.A.; Cusumano, C.; Fujioka, A.; Lim-Fong, G.; Patterson, P.; Pogliano, J. Treadmilling of a
568 prokaryotic tubulin-like protein, TubZ, required for plasmid stability in *Bacillus thuringiensis*. *Genes Dev.*
569 **2007**, *21*, 1340–1352.
57048. Delbrück, H.; Ziegelin, G.; Lanka, E.; Heinemann, U. An Src homology 3-like domain is responsible for
571 dimerization of the repressor protein KorB encoded by the promiscuous IncP plasmid RP4. *J. Biol. Chem.*
572 **2002**, *277*, 4191–4198.
57349. Khare, D.; Ziegelin, G.; Lanka, E.; Heinemann, U. Sequence-specific DNA binding determined by contacts
574 outside the helix-turn-helix motif of the ParB homolog KorB. *Nat. Struct. Mol. Biol.* **2004**, *11*, 656–663.
57550. Schumacher, M.A.; Mansoor, A.; Funnell, B.E. Structure of a four-way bridged ParB-DNA complex
576 provides insight into P1 segrosome assembly. *J. Biol. Chem.* **2007**, *282*, 10456–10464.
57751. Schumacher, M.A.; Piro, K.M.; Xu, W. Insight into F plasmid DNA segregation revealed by structures of
578 SopB and SopB-DNA complexes. *Nucleic Acids Res.* **2010**, *38*, 4514–4526.
57952. Golovanov, A.P.; Barillà, D.; Golovanova, M.; Hayes, F.; Lian, L.-Y. ParG, a protein required for active
580 partition of bacterial plasmids, has a dimeric ribbon-helix-helix structure. *Mol. Microbiol.* **2003**, *50*, 1141–
581 1153.
58253. Murayama, K.; Orth, P.; de la Hoz, A.B.; Alonso, J.C.; Saenger, W. Crystal structure of omega transcriptional
583 repressor encoded by *Streptococcus pyogenes* plasmid pSM19035 at 1.5 Å resolution. *J. Mol. Biol.* **2001**, *314*,
584 789–796.
58554. Barillà, D.; Carmelo, E.; Hayes, F. The tail of the ParG DNA segregation protein remodels ParF polymers
586 and enhances ATP hydrolysis via an arginine finger-like motif. *Proc. Natl. Acad. Sci. USA* **2007**, *104*, 1811–
587 1816.
58855. Ni, L.; Xu, W.; Kumaraswami, M.; Schumacher, M.A. Plasmid protein TubR uses a distinct mode of HTH-
589 DNA binding and recruits the prokaryotic tubulin homolog TubZ to effect DNA partition. *Proc. Natl. Acad.*
590 *Sci. USA* **2010**, *107*, 11763–11768.
- 591 56. Baxter, J.C.; Funnell, B.E. Plasmid partition mechanisms in Plasmids. *Biology and Impact in*
592 *Biotechnology and Discovery*, eds M. E. Tolmasky, and J. A. Alonso, (Washington, DC: ASM Press)
593 **2015**, 135–155.
59457. Schumacher, M.A. Bacterial plasmid partition machinery: A minimalist approach to survival. *Curr. Opin.*
595 *Struct. Biol.* **2012**, *22*, 72–79.

59658. Ogasawara, N.; Yoshikawa, H. Genes and their organization in the replication origin region of the bacterial chromosome. *Mol. Microbiol.* **1992**, *6*, 629–634.
59859. Livny, J.; Yamaichi, Y.; Waldor, M.K. Distribution of centromere-like *parS* sites in bacteria: Insights from comparative genomics. *J. Bacteriol.* **2007**, *189*, 8693–8703.
60060. Gal-Mor, O.; Borovok, I.; Av-Gay, Y.; Cohen, G.; Aharonowitz, Y. Gene organization in the *trxA/B-oriC* region of the *Streptomyces coelicolor* chromosome and comparison with other eubacteria. *Gene* **1998**, *217*, 83–90.
60361. Lin, D.C.; Grossman, A.D. Identification and characterization of a bacterial chromosome partitioning site. *Cell* **1998**, *92*, 675–685.
60562. Yamaichi, Y.; Niki, H. Active segregation by the *Bacillus subtilis* partitioning system in *Escherichia coli*. *Proc. Natl. Acad. Sci. USA* **2000**, *97*, 14656–14661.
60763. Godfrin-Estevenson, A.-M.; Pasta, F.; Lane, D. The *parAB* gene products of *Pseudomonas putida* exhibit partition activity in both *P. putida* and *Escherichia coli*. *Mol. Microbiol.* **2002**, *43*, 39–49.
60964. Bartosik, A.A.; Lasocki, K.; Mierzejewska, J.; Thomas, C.M.; Jagura-Burdzy, G. ParB of *Pseudomonas aeruginosa*: Interactions with its partner ParA and its target *parS* and specific effects on bacterial growth. *J. Bacteriol.* **2004**, *186*, 6983–6998.
61265. Lemon, K.P.; Grossman, A.D. Localization of bacterial DNA polymerase: Evidence for a factory model of replication. *Science* **1998**, *282*, 1516–1519.
61466. Sawitzke, J.; Austin, S. An analysis of the factory model for chromosome replication and segregation in bacteria. *Mol. Microbiol.* **2001**, *40*, 786–794.
61667. Bartosik, A.A.; Jagura-Burdzy, G. Bacterial chromosome segregation. *Acta Biochim. Pol.* **2005**, *52*, 1–34.
61768. Breier, A.M.; Grossman, A.D. Whole-genome analysis of the chromosome partitioning and sporulation protein Spo0J (ParB) reveals spreading and origin-distal sites on the *Bacillus subtilis* chromosome. *Mol. Microbiol.* **2007**, *64*, 703–718.
62069. Ireton, K.; Gunther, N.W.; Grossman, A.D. *spo0J* is required for normal chromosome segregation as well as the initiation of sporulation in *Bacillus subtilis*. *J. Bacteriol.* **1994**, *176*, 5320–5329.
62270. Lee, P.S.; Grossman, A.D. The chromosome partitioning proteins Soj (ParA) and Spo0J (ParB) contribute to accurate chromosome partitioning, separation of replicated sister origins, and regulation of replication initiation in *Bacillus subtilis*. *Mol. Microbiol.* **2006**, *60*, 853–869.
62571. Minnen, A.; Attaiech, L.; Thon, M.; Gruber, S.; Veening, J.-W. SMC is recruited to *oriC* by ParB and promotes chromosome segregation in *Streptococcus pneumoniae*. *Mol. Microbiol.* **2011**, *81*, 676–688.
62772. Böhm, K.; Giacomelli, G.; Schmidt, A.; Imhof, A.; Koszul, R.; Marbouty, M.; Bramkamp, M. Chromosome organization by a conserved condensin-ParB system in the actinobacterium *Corynebacterium glutamicum*. *bioRxiv* **2019**, doi: 10.1101/649749.
63073. Donovan, C.; Schwaiger, A.; Krämer, R.; Bramkamp, M. Subcellular localization and characterization of the ParAB system from *Corynebacterium glutamicum*. *J. Bacteriol.* **2010**, *192*, 3441–3451.
63274. Jakimowicz, D.; Brzostek, A.; Rumijowska-Galewicz, A.; Zydek, P.; Dołzbłasz, A.; Smulczyk-Krawczynszyn, A.; Zimniak, T.; Wojtasz, L.; Zawilak-Pawlik, A.; Kois, A.; et al. Characterization of the mycobacterial chromosome segregation protein ParB and identification of its target in *Mycobacterium smegmatis*. *Microbiol. Read. Engl.* **2007**, *153*, 4050–4060.
63675. Santi, I.; McKinney, J.D. Chromosome organization and replisome dynamics in *Mycobacterium smegmatis*. *mBio* **2015**, *6*, e01999-14, doi:10.1128/mBio.01999-14.
63876. Jakimowicz, D.; Chater, K.; Zakrzewska-Czerwińska, J. The ParB protein of *Streptomyces coelicolor* A3(2) recognizes a cluster of *parS* sequences within the origin-proximal region of the linear chromosome. *Mol. Microbiol.* **2002**, *45*, 1365–1377.
64177. Kim, H.J.; Calcutt, M.J.; Schmidt, F.J.; Chater, K.F. Partitioning of the linear chromosome during sporulation of *Streptomyces coelicolor* A3(2) involves an *oriC*-linked *parAB* locus. *J. Bacteriol.* **2000**, *182*, 1313–1320.
64378. Jakimowicz, D.; Zydek, P.; Kois, A.; Zakrzewska-Czerwińska, J.; Chater, K.F. Alignment of multiple chromosomes along helical ParA scaffolding in sporulating *Streptomyces hyphae*. *Mol. Microbiol.* **2007**, *65*, 625–641.
64679. Donczew, M.; Mackiewicz, P.; Wróbel, A.; Flärdh, K.; Zakrzewska-Czerwińska, J.; Jakimowicz, D. ParA and ParB coordinate chromosome segregation with cell elongation and division during *Streptomyces* sporulation. *Open Biol.* **2016**, *6*, 150263, doi:10.1098/rsob.150263.

64980. Tran, N.T.; Stevenson, C.E.; Som, N.F.; Thanapipatsiri, A.; Jalal, A.S.B.; Le, T.B.K. Permissive zones for the
650 centromere-binding protein ParB on the *Caulobacter crescentus* chromosome. *Nucleic Acids Res.* **2018**, *46*,
651 1196–1209.
65281. Toro, E.; Hong, S.-H.; McAdams, H.H.; Shapiro, L. *Caulobacter* requires a dedicated mechanism to initiate
653 chromosome segregation. *Proc. Natl. Acad. Sci. USA* **2008**, *105*, 15435–15440.
65482. Mohl, D.A.; Easter, J.; Gober, J.W. The chromosome partitioning protein, ParB, is required for cytokinesis
655 in *Caulobacter crescentus*. *Mol. Microbiol.* **2001**, *42*, 741–755.
65683. Jung, A.; Raßbach, A.; Pulpetta, R.L.; van Teeseling, M.C.F.; Heinrich, K.; Sobetzko, P.; Serrania, J.; Becker,
657 A.; Thanbichler, M. Two-step chromosome segregation in the stalked budding bacterium *Hyphomonas*
658 *neptunium*. *Nat. Commun.* **2019**, *10*, 3290, doi:10.1038/s41467-019-11242-5.
65984. Dubarry, N.; Pasta, F.; Lane, D. ParABS systems of the four replicons of *Burkholderia cenocepacia*: New
660 chromosome centromeres confer partition specificity. *J. Bacteriol.* **2006**, *188*, 1489–1496.
66185. Du, W.-L.; Dubarry, N.; Passot, F.M.; Kamgoué, A.; Murray, H.; Lane, D.; Pasta, F. Orderly Replication and
662 segregation of the four replicons of *Burkholderia cenocepacia* J2315. *PLoS Genet.* **2016**, *12*, e1006172,
663 doi:10.1371/journal.pgen.1006172.
66486. Passot, F.M.; Calderon, V.; Fichant, G.; Lane, D.; Pasta, F. Centromere binding and evolution of
665 chromosomal partition systems in the Burkholderiales. *J. Bacteriol.* **2012**, *194*, 3426–3436.
66687. Pillet, F.; Passot, F.M.; Pasta, F.; Anton Leberre, V.; Bouet, J.-Y. Analysis of ParB-centromere interactions by
667 multiplex SPR imaging reveals specific patterns for binding ParB in six centromeres of Burkholderiales
668 chromosomes and plasmids. *PLoS ONE* **2017**, *12*, e0177056, doi:10.1371/journal.pone.0177056.
66988. Iniesta, A.A. ParABS system in chromosome partitioning in the bacterium *Myxococcus xanthus*. *PLoS ONE*
670 **2014**, *9*, e86897, doi:10.1371/journal.pone.0086897.
67189. Lagage, V.; Boccard, F.; Vallet-Gely, I. Regional control of chromosome segregation in *Pseudomonas*
672 *aeruginosa*. *PLoS Genet.* **2016**, *12*, e1006428, doi:10.1371/journal.pgen.1006428.
67390. Kawalek, A.; Bartosik, A.A.; Glabski, K.; Jagura-Burdzy, G. *Pseudomonas aeruginosa* partitioning protein
674 ParB acts as a nucleoid-associated protein binding to multiple copies of a *parS*-related motif. *Nucleic Acids*
675 *Res.* **2018**, *46*, 4592–4606.
67691. Jecz, P.; Bartosik, A.A.; Glabski, K.; Jagura-Burdzy, G. A single *parS* sequence from the cluster of four sites
677 closest to *oriC* is necessary and sufficient for proper chromosome segregation in *Pseudomonas aeruginosa*.
678 *PLoS ONE* **2015**, *10*, e0120867, doi:10.1371/journal.pone.0120867.
67992. Bartosik, A.A.; Mierzejewska, J.; Thomas, C.M.; Jagura-Burdzy, G. ParB deficiency in *Pseudomonas*
680 *aeruginosa* destabilizes the partner protein ParA and affects a variety of physiological parameters.
681 *Microbiology* **2009**, *155*, 1080–1092.
68293. Lewis, R.A.; Bignell, C.R.; Zeng, W.; Jones, A.C.; Thomas, C.M. Chromosome loss from *par* mutants of
683 *Pseudomonas putida* depends on growth medium and phase of growth. *Microbiology* **2002**, *148*, 537–548.
68494. Yamaichi, Y.; Fogel, M.A.; McLeod, S.M.; Hui, M.P.; Waldor, M.K. Distinct centromere-like *parS* sites on
685 the two chromosomes of *Vibrio* spp. *J. Bacteriol.* **2007**, *189*, 5314–5324.
68695. Kadoya, R.; Baek, J.H.; Sarker, A.; Chattoraj, D.K. Participation of chromosome segregation protein ParAI
687 of *Vibrio cholerae* in chromosome replication. *J. Bacteriol.* **2011**, *193*, 1504–1514.
68896. Charaka, V.K.; Misra, H.S. Functional characterization of the role of the chromosome I partitioning system
689 in genome segregation in *Deinococcus radiodurans*. *J. Bacteriol.* **2012**, *194*, 5739–5748.
69097. Li, H.; Angelov, A.; Pham, V.T.T.; Leis, B.; Liebl, W. Characterization of chromosomal and megaplasmid
691 partitioning loci in *Thermus thermophilus* HB27. *BMC Genomics* **2015**, *16*, 317.
69298. Li, H. Random chromosome partitioning in the polyploid bacterium *Thermus thermophilus* HB27. *G3 Genes*
693 *Genomes Genet.* **2019**, *9*, 1249–1261.
69499. Mori, H.; Mori, Y.; Ichinose, C.; Niki, H.; Ogura, T.; Kato, A.; Hiraga, S. Purification and characterization of
695 SopA and SopB proteins essential for F plasmid partitioning. *J. Biol. Chem.* **1989**, *264*, 15535–15541.
696100. Hayes, F.; Radnedge, L.; Davis, M.A.; Austin, S.J. The homologous operons for P1 and P7 plasmid partition
697 are autoregulated from dissimilar operator sites. *Mol. Microbiol.* **1994**, *11*, 249–260.
698101. Hester, C.M.; Lutkenhaus, J. Soj (ParA) DNA binding is mediated by conserved arginines and is essential
699 for plasmid segregation. *Proc. Natl. Acad. Sci. USA* **2007**, *104*, 20326–20331.
700102. Chu, C.-H.; Yen, C.-Y.; Chen, B.-W.; Lin, M.-G.; Wang, L.-H.; Tang, K.-Z.; Hsiao, C.-D.; Sun, Y.-J. Crystal
701 structures of HpSoj-DNA complexes and the nucleoid-adaptor complex formation in chromosome
702 segregation. *Nucleic Acids Res.* **2019**, *47*, 2113–2129.

703103. Ptacin, J.L.; Lee, S.F.; Garner, E.C.; Toro, E.; Eckart, M.; Comolli, L.R.; Moerner, W.E.; Shapiro, L. A spindle-
704 like apparatus guides bacterial chromosome segregation. *Nat. Cell Biol.* **2010**, *12*, 791–798.
705104. Figge, R.M.; Easter, J.; Gober, J.W. Productive interaction between the chromosome partitioning proteins,
706 ParA and ParB, is required for the progression of the cell cycle in *Caulobacter crescentus*. *Mol. Microbiol.* **2003**,
707 *47*, 1225–1237.
708105. Bartosik, A.A.; Glabski, K.; Jecz, P.; Lasocki, K.; Mikosa, M.; Plochocka, D.; Thomas, C.M.; Jagura-Burdzy,
709 G. Dissection of the region of *Pseudomonas aeruginosa* ParA that is important for dimerization and
710 interactions with its partner ParB. *Microbiology* **2014**, *160*, 2406–2420.
711106. Ringgaard, S.; Zon, J.; van; Howard, M.; Gerdes, K. Movement and equipositioning of plasmids by ParA
712 filament disassembly. *Proc. Natl. Acad. Sci. USA* **2009**, *106*, 19369–19374.
713107. Fogel, M.A.; Waldor, M.K. A dynamic, mitotic-like mechanism for bacterial chromosome segregation.
714 *Genes Dev.* **2006**, *20*, 3269–3282.
715108. Hui, M.P.; Galkin, V.E.; Yu, X.; Stasiak, A.Z.; Stasiak, A.; Waldor, M.K.; Egelman, E.H. ParA2, a *Vibrio*
716 *cholerae* chromosome partitioning protein, forms left-handed helical filaments on DNA. *Proc. Natl. Acad.*
717 *Sci. USA* **2010**, *107*, 4590–4595.
718109. Lim, H.C.; Surovtsev, I.V.; Beltran, B.G.; Huang, F.; Bewersdorf, J.; Jacobs-Wagner, C. Evidence for a DNA-
719 relay mechanism in ParABS-mediated chromosome segregation. *Elife* **2014**, *3*, e02758,
720 doi:10.7554/eLife.02758.
721110. Vecchiarelli, A.G.; Mizuuchi, K.; Funnell, B.E. Surfing biological surfaces: Exploiting the nucleoid for
722 partition and transport in bacteria. *Mol. Microbiol.* **2012**, *86*, 513–523.
723111. Hwang, L.C.; Vecchiarelli, A.G.; Han, Y.-W.; Mizuuchi, M.; Harada, Y.; Funnell, B.E.; Mizuuchi, K. ParA-
724 mediated plasmid partition driven by protein pattern self-organization. *EMBO J.* **2013**, *32*, 1238–1249.
725112. Kisner, J.R.; Kuwada, N.J. Nucleoid-mediated positioning and transport in bacteria. *Curr. Genet.* **2019**,
726 doi:10.1007/s00294-019-01041-2.
727113. Brooks, A.C.; Hwang, L.C. Reconstitutions of plasmid partition systems and their mechanisms. *Plasmid*
728 **2017**, *91*, 37–41.
729114. Kusiak, M.; Gapczyńska, A.; Plochocka, D.; Thomas, C.M.; Jagura-Burdzy, G. Binding and spreading of
730 ParB on DNA determine its biological function in *Pseudomonas aeruginosa*. *J. Bacteriol.* **2011**, *193*, 3342–3355.
731115. Leonard, T.A.; Butler, P.J.G.; Löwe, J. Structural analysis of the chromosome segregation protein Spo0J from
732 *Thermus thermophilus*. *Mol. Microbiol.* **2004**, *53*, 419–432.
733116. Chen, B.-W.; Lin, M.-H.; Chu, C.-H.; Hsu, C.-E.; Sun, Y.-J. Insights into ParB spreading from the complex
734 structure of Spo0J and *parS*. *Proc. Natl. Acad. Sci. USA* **2015**, *112*, 6613–6618.
735117. Graham, T.G.W.; Wang, X.; Song, D.; Etson, C.M.; van Oijen, A.M.; Rudner, D.Z.; Loparo, J.J. ParB
736 spreading requires DNA bridging. *Genes Dev.* **2014**, *28*, 1228–1238.
737118. Funnell, B.E. ParB partition proteins: Complex formation and spreading at bacterial and plasmid
738 centromeres. *Front. Mol. Biosci.* **2016**, *3*, 44, doi:10.3389/fmolb.2016.00044.
739119. Fisher, G.L.; Pastrana, C.L.; Higman, V.A.; Koh, A.; Taylor, J.A.; Butterer, A.; Craggs, T.; Sobott, F.; Murray,
740 H.; Crump, M.P.; et al. The structural basis for dynamic DNA binding and bridging interactions which
741 condense the bacterial centromere. *ELife* **2017**, *6*, e28086, doi:10.7554/eLife.28086.
742120. Taylor, J.A.; Pastrana, C.L.; Butterer, A.; Pernstich, C.; Gwynn, E.J.; Sobott, F.; Moreno-Herrero, F.;
743 Dillingham, M.S. Specific and non-specific interactions of ParB with DNA: Implications for chromosome
744 segregation. *Nucleic Acids Res.* **2015**, *43*, 719–731.
745121. Madariaga-Marcos, J.; Pastrana, C.L.; Fisher, G.L.; Dillingham, M.S.; Moreno-Herrero, F. ParB dynamics
746 and the critical role of the CTD in DNA condensation unveiled by combined force-fluorescence
747 measurements. *ELife* **2019**, *8*, e43812, doi:10.7554/eLife.43812.
748122. Soh, Y.-M.; Davidson, I.F.; Zamuner, S.; Basquin, J.; Bock, F.P.; Taschner, M.; Veening, J.-W.; Rios, P.D.L.;
749 Peters, J.-M.; Gruber, S. Self-organization of *parS* centromeres by the ParB CTP hydrolase. *Science* **2019**, *366*,
750 1129–1133.
751123. Lynch, A.S.; Wang, J.C. SopB protein-mediated silencing of genes linked to the *sopC* locus of *Escherichia coli*
752 F plasmid. *Proc. Natl. Acad. Sci. USA* **1995**, *92*, 1896–1900.
753124. Rodionov, O.; Łobocka, M.; Yarmolinsky, M. Silencing of genes flanking the P1 plasmid centromere. *Science*
754 **1999**, *283*, 546–549.
755125. Lukaszewicz, M.; Kostelidou, K.; Bartosik, A.A.; Cooke, G.D.; Thomas, C.M.; Jagura-Burdzy, G. Functional
756 dissection of the ParB homologue (KorB) from IncP-1 plasmid RK2. *Nucleic Acids Res.* **2002**, *30*, 1046–1055.

757126. Bingle, L.E.H.; Macartney, D.P.; Fantozzi, A.; Manzoor, S.E.; Thomas, C.M. Flexibility in repression and
758 cooperativity by KorB of broad host range IncP-1 plasmid RK2. *J. Mol. Biol.* **2005**, *349*, 302–316.
759127. Mohl, D.A.; Gober, J.W. Cell cycle-dependent polar localization of chromosome partitioning proteins in
760 *Caulobacter crescentus*. *Cell* **1997**, *88*, 675–684.
761128. Lin, D.C.-H.; Levin, P.A.; Grossman, A.D. Bipolar localization of a chromosome partition protein in *Bacillus*
762 *subtilis*. *Proc. Natl. Acad. Sci. USA* **1997**, *94*, 4721–4726.
763129. Debaugny, R.E.; Sanchez, A.; Rech, J.; Labourdette, D.; Dorignac, J.; Geniet, F.; Palmeri, J.; Parmeggiani, A.;
764 Boudsocq, F.; Anton Leberre, V.; et al. A conserved mechanism drives partition complex assembly on
765 bacterial chromosomes and plasmids. *Mol. Syst. Biol.* **2018**, *14*, e8516, doi:10.15252/msb.20188516.
766130. Attaiech, L.; Minnen, A.; Kjos, M.; Gruber, S.; Veening, J.-W. The ParB-*parS* chromosome segregation
767 system modulates competence development in *Streptococcus pneumoniae*. *mBio* **2015**, *6*, e00662,
768 doi:10.1128/mBio.00662-15.
769131. Glaser, P.; Sharpe, M.E.; Raether, B.; Perego, M.; Ohlsen, K.; Errington, J. Dynamic, mitotic-like behavior of
770 a bacterial protein required for accurate chromosome partitioning. *Genes Dev.* **1997**, *11*, 1160–1168.
771132. Baek, J.H.; Rajagopala, S.V.; Chatteraj, D.K. Chromosome segregation proteins of *Vibrio cholerae* as
772 transcription regulators. *mBio* **2014**, *5*, e01061–e01014, doi:10.1128/mBio.01061-14.
773133. Jalal, A.S.B.; Pastrana, C.L.; Tran, N.T.; Stevenson, C.E.; Lawson, D.M.; Moreno-Herrero, F.; Le, T.B.K.
774 Structural and biochemical analyses of *Caulobacter crescentus* ParB reveal the role of its N-terminal domain
775 in chromosome segregation. *bioRxiv* **2019**, 816959, doi:10.1101/816959.
776134. Song, D.; Rodrigues, K.; Graham, T.G.W.; Loparo, J.J. A network of *cis* and *trans* interactions is required for
777 ParB spreading. *Nucleic Acids Res.* **2017**, *45*, 7106–7117.
778135. Chaudhuri, B.N.; Dean, R. The evidence of large-scale DNA-induced compaction in the *Mycobacterial*
779 chromosomal ParB. *J. Mol. Biol.* **2011**, *413*, 901–907.
780136. Broedersz, C.P.; Wang, X.; Meir, Y.; Loparo, J.J.; Rudner, D.Z.; Wingreen, N.S. Condensation and
781 localization of the partitioning protein ParB on the bacterial chromosome. *Proc. Natl. Acad. Sci. USA* **2014**,
782 *111*, 8809–8814.
783137. Audibert, S.; Gac, N.T.-L.; Rech, J.; Turlan, C.; Bouet, J.-Y.; Bystricky, K.; Lane, D. Role of centromere sites
784 in activation of ParB proteins for partition complex assembly. *bioRxiv* **2019**, 862136, doi:10.1101/862136.
785138. Walter, J.-C.; Walliser, N.-O.; David, G.; Dorignac, J.; Geniet, F.; Palmeri, J.; Parmeggiani, A.; Wingreen,
786 N.S.; Broedersz, C.P. Looping and clustering model for the organization of protein-DNA complexes on the
787 bacterial genome. *N. J. Phys.* **2018**, *20*, e035002, doi:10.1073/pnas.1302950110.
788139. Sanchez, A.; Cattoni, D.I.; Walter, J.-C.; Rech, J.; Parmeggiani, A.; Nollmann, M.; Bouet, J.-Y. Stochastic Self-
789 Assembly of ParB proteins builds the bacterial DNA segregation apparatus. *Cell Syst.* **2015**, *1*, 163–173.
790140. Jalal, A.S.B.; Tran, N.T.; Le, T.B.K. ParB spreading on DNA requires cytidine triphosphate *in vitro*. *bioRxiv*
791 **2019**, 865972, doi:10.1101/2019.12.11.865972.
792141. Osorio-Valeriano, M.; Altegoer, F.; Steinchen, W.; Urban, S.; Liu, Y.; Bange, G.; Thanbichler, M. ParB-type
793 DNA segregation proteins are CTP-dependent molecular switches. *Cell* **2019**, *179*, 1512–1524.e15.
794142. Jalal, A.S.B.; Tran, N.T.; Stevenson, C.E.; Tan, X.; Lawson, D.M.; Le, T.B.K. Evolving a new protein-DNA
795 interface via sequential introduction of permissive and specificity-switching mutations. *bioRxiv* **2019**,
796 724823, doi:10.1101/724823.
797143. Chen, S.; Zhou, Y.; Chen, Y.; Gu, J. Fastp: An ultra-fast all-in-one FASTQ preprocessor. *Bioinformatics* **2018**,
798 *34*, i884–i890.
799144. Langmead, B.; Salzberg, S.L. Fast gapped-read alignment with Bowtie 2. *Nat. Methods* **2012**, *9*, 357–359.
800145. Li, H. A statistical framework for SNP calling, mutation discovery, association mapping and population
801 genetical parameter estimation from sequencing data. *Bioinforma. Oxf. Engl.* **2011**, *27*, 2987–2993.
802146. Ramírez, F.; Ryan, D.P.; Grüning, B.; Bhardwaj, V.; Kilpert, F.; Richter, A.S.; Heyne, S.; Dündar, F.; Manke,
803 T. deepTools2: A next generation web server for deep-sequencing data analysis. *Nucleic Acids Res.* **2016**, *44*,
804 W160–W165.
805147. Yuen, K.C.; Gerton, J.L. Taking cohesin and condensin in context. *PLoS Genet.* **2018**, *14*, e1007118,
806 doi:10.1371/journal.pgen.1007118.
807148. Minnen, A.; Bürmann, F.; Wilhelm, L.; Anchimiuk, A.; Diebold-Durand, M.-L.; Gruber, S. Control of Smc
808 coiled coil architecture by the ATPase heads facilitates targeting to chromosomal ParB/*parS* and release
809 onto flanking DNA. *Cell Rep.* **2016**, *14*, 2003–2016.

810149. Wang, X.; Brandão, H.B.; Le, T.B.K.; Laub, M.T.; Rudner, D.Z. *Bacillus subtilis* SMC complexes juxtapose
811 chromosome arms as they travel from origin to terminus. *Science* **2017**, *355*, 524–527.
812150. Hirano, T. At the heart of the chromosome: SMC proteins in action. *Nat. Rev. Mol. Cell Biol.* **2006**, *7*, 311–
813 322.
814151. Tran, N.T.; Laub, M.T.; Le, T.B.K. SMC Progressively aligns chromosomal arms in *Caulobacter crescentus* but
815 is antagonized by convergent transcription. *Cell Rep.* **2017**, *20*, 2057–2071.
816152. Wilhelm, L.; Bürmann, F.; Minnen, A.; Shin, H.-C.; Toseland, C.P.; Oh, B.-H.; Gruber, S. SMC condensin
817 entraps chromosomal DNA by an ATP hydrolysis dependent loading mechanism in *Bacillus subtilis*. *eLife*
818 **2015**, *4*, e06659, doi:10.7554/eLife.06659.
819153. Hassler, M.; Shaltiel, I.A.; Kschonsak, M.; Simon, B.; Merkel, F.; Thärichen, L.; Bailey, H.J.; Macošek, J.;
820 Bravo, S.; Metz, J.; et al. Structural basis of an asymmetric condensin ATPase cycle. *Mol. Cell* **2019**, *74*, 1175–
821 1188, doi:10.1016/j.molcel.2019.03.037.
822154. Gruber, S. SMC complexes sweeping through the chromosome: Going with the flow and against the tide.
823 *Curr. Opin. Microbiol.* **2018**, *42*, 96–103.
824155. Nolivos, S.; Upton, A.L.; Badrinarayanan, A.; Müller, J.; Zawadzka, K.; Wiktor, J.; Gill, A.; Arciszewska, L.;
825 Nicolas, E.; Sherratt, D. MatP regulates the coordinated action of topoisomerase IV and MukBEF in
826 chromosome segregation. *Nat. Commun.* **2016**, *7*, 10466.
827156. Zhao, H.; Clevenger, A.L.; Ritchey, J.W.; Zgurskaya, H.I.; Rybenkov, V.V. *Pseudomonas aeruginosa*
828 condensins support opposite differentiation states. *J. Bacteriol.* **2016**, *198*, 2936–2944.
829157. Panas, M.W.; Jain, P.; Yang, H.; Mitra, S.; Biswas, D.; Wattam, A.R.; Letvin, N.L.; Jacobs, W.R. Noncanonical
830 SMC protein in *Mycobacterium smegmatis* restricts maintenance of *Mycobacterium fortuitum* plasmids. *Proc.*
831 *Natl. Acad. Sci. USA* **2014**, *111*, 13264–13271.
832158. Szafran, M.; Skut, P.; Ditekowski, B.; Ginda, K.; Chandra, G.; Zakrzewska-Czerwińska, J.; Jakimowicz, D.
833 Topoisomerase I (TopA) is recruited to ParB complexes and is required for proper chromosome
834 organization during *Streptomyces coelicolor* sporulation. *J. Bacteriol.* **2013**, *195*, 4445–4455.
835159. Champoux, J.J. DNA topoisomerases: Structure, function, and mechanism. *Annu. Rev. Biochem.* **2001**, *70*,
836 369–413.
837160. Murray, H.; Errington, J. Dynamic control of the DNA replication initiation protein DnaA by Soj/ParA. *Cell*
838 **2008**, *135*, 74–84.
839161. Scholefield, G.; Whiting, R.; Errington, J.; Murray, H. Spo0J regulates the oligomeric state of Soj to trigger
840 its switch from an activator to an inhibitor of DNA replication initiation. *Mol. Microbiol.* **2011**, *79*, 1089–1100.
841162. Scholefield, G.; Errington, J.; Murray, H. Soj/ParA stalls DNA replication by inhibiting helix formation of
842 the initiator protein DnaA. *EMBO J.* **2012**, *31*, 1542–1555.
843163. Maurya, G.K.; Kota, S.; Misra, H.S. Characterisation of ParB encoded on multipartite genome in *Deinococcus*
844 *radiodurans* and their roles in radioresistance. *Microbiol. Res.* **2019**, *223*, 22–32.
845164. Perry, S.E.; Edwards, D.H. The *Bacillus subtilis* DivIVA protein has a sporulation-specific proximity to
846 Spo0J. *J. Bacteriol.* **2006**, *188*, 6039–6043.
847165. Lin, L.; Osorio Valeriano, M.; Harms, A.; Søgaard-Andersen, L.; Thanbichler, M. Bactofilin-mediated
848 organization of the ParABS chromosome segregation system in *Myxococcus xanthus*. *Nat. Commun.* **2017**, *8*,
849 1817, doi:10.1038/s41467-017-02015-z.
850166. Ginda, K.; Bezulska, M.; Ziółkiewicz, M.; Dziadek, J.; Zakrzewska-Czerwińska, J.; Jakimowicz, D. ParA of
851 *Mycobacterium smegmatis* co-ordinates chromosome segregation with the cell cycle and interacts with the
852 polar growth determinant DivIVA. *Mol. Microbiol.* **2013**, *87*, 998–1012.
853167. Pióro, M.; Małecki, T.; Portas, M.; Magierowska, I.; Trojanowski, D.; Sherratt, D.; Zakrzewska-Czerwińska,
854 J.; Ginda, K.; Jakimowicz, D. Competition between DivIVA and the nucleoid for ParA binding promotes
855 segrosome separation and modulates mycobacterial cell elongation. *Mol. Microbiol.* **2019**, *111*, 204–220.
856168. Nourikyan, J.; Kjos, M.; Mercy, C.; Cluzel, C.; Morlot, C.; Noirot-Gros, M.-F.; Guiral, S.; Lavergne, J.-P.;
857 Veening, J.-W.; Grangeasse, C. Autophosphorylation of the bacterial tyrosine-kinase CpsD connects
858 capsule synthesis with the cell cycle in *Streptococcus pneumoniae*. *PLoS Genet.* **2015**, *11*, e1005518,
859 doi:10.1371/journal.pgen.1005518.
860169. Fadda, D.; Santona, A.; D’Ulisse, V.; Ghelardini, P.; Ennas, M.G.; Whalen, M.B.; Massidda, O. *Streptococcus*
861 *pneumoniae* DivIVA: Localization and interactions in a MinCD-free context. *J. Bacteriol.* **2007**, *189*, 1288–1298.

862170. Mercy, C.; Ducret, A.; Slager, J.; Laverigne, J.-P.; Freton, C.; Nagarajan, S.N.; Garcia, P.S.; Noirot-Gros, M.-
863 F.; Dubarry, N.; Nourikyan, J.; et al. RocS drives chromosome segregation and nucleoid protection in
864 *Streptococcus pneumoniae*. *Nat. Microbiol.* **2019**, *4*, 1661–1670.
865171. Kois-Ostrowska, A.; Strzałka, A.; Lipietta, N.; Tilley, E.; Zakrzewska-Czerwińska, J.; Herron, P.;
866 Jakimowicz, D. Unique function of the bacterial chromosome segregation machinery in apically growing
867 *Streptomyces*—targeting the chromosome to new hyphal tubes and its anchorage at the tips. *PLoS Genet.*
868 **2016**, *12*, e1006488, doi:10.1371/journal.pgen.1006488.
869172. Ditkowski, B.; Troć, P.; Ginda, K.; Donczew, M.; Chater, K.F.; Zakrzewska-Czerwińska, J.; Jakimowicz, D.
870 The actinobacterial signature protein ParJ (SCO1662) regulates ParA polymerization and affects
871 chromosome segregation and cell division during *Streptomyces* sporulation. *Mol. Microbiol.* **2010**, *78*, 1403–
872 1415.
873173. Ditkowski, B.; Holmes, N.; Rydzak, J.; Donczew, M.; Bezulska, M.; Ginda, K.; Kedzierski, P.; Zakrzewska-
874 Czerwińska, J.; Kelemen, G.H.; Jakimowicz, D. Dynamic interplay of ParA with the polarity protein, Scy,
875 coordinates the growth with chromosome segregation in *Streptomyces coelicolor*. *Open Biol.* **2013**, *3*, 130006,
876 doi:10.1098/rsob.130006.
877174. Shebelut, C.W.; Guberman, J.M.; Teeffelen, S.; van; Yakhnina, A.A.; Gitai, Z. *Caulobacter* chromosome
878 segregation is an ordered multistep process. *Proc. Natl. Acad. Sci. USA* **2010**, *107*, 14194–14198.
879175. Bowman, G.R.; Comolli, L.R.; Zhu, J.; Eckart, M.; Koenig, M.; Downing, K.H.; Moerner, W.E.; Earnest, T.;
880 Shapiro, L. A polymeric protein anchors the chromosomal origin/ParB complex at a bacterial cell pole. *Cell*
881 **2008**, *134*, 945–955.
882176. Ptacin, J.L.; Gahlmann, A.; Bowman, G.R.; Perez, A.M.; von Diezmann, A.R.S.; Eckart, R.M.; Moerner, W.E.;
883 Shapiro, L. Bacterial scaffold directs pole-specific centromere segregation. *Proc. Natl. Acad. Sci. USA* **2014**,
884 *111*, 2046–2055.
885177. Thanbichler, M.; Shapiro, L. MipZ, A spatial regulator coordinating chromosome segregation with cell
886 division in *Caulobacter*. *Cell* **2006**, *126*, 147–162.
887178. Schofield, W.B.; Lim, H.C.; Jacobs-Wagner, C. Cell cycle coordination and regulation of bacterial
888 chromosome segregation dynamics by polarly localized proteins. *EMBO J.* **2010**, *29*, 3068–3081.
889179. Charaka, V.; Kota, S.; Misra, H. ParA encoded on chromosome i of *Deinococcus radiodurans* requires its
890 cognate ParB and centromere for its dynamics. *Proc. Indian Natl. Sci. Acad.* **2014**, *80*, 663,
891 doi:10.16943/ptinsa/2014/v80i3/55141.
892180. Maurya, G.K.; Modi, K.; Misra, H.S. Divisome and segrosome components of *Deinococcus radiodurans*
893 interact through cell division regulatory proteins. *Microbiol. Read. Engl.* **2016**, *162*, 1321–1334.
894181. Chaudhary, R.; Gupta, A.; Kota, S.; Misra, H.S. N-terminal domain of DivIVA contributes to its
895 dimerization and interaction with genome segregation proteins in a radioresistant bacterium *Deinococcus*
896 *radiodurans*. *Int. J. Biol. Macromol.* **2019**, *128*, 12–21.
897182. Yamaichi, Y.; Bruckner, R.; Ringgaard, S.; Möll, A.; Cameron, D.E.; Briegel, A.; Jensen, G.J.; Davis, B.M.;
898 Waldor, M.K. A multidomain hub anchors the chromosome segregation and chemotactic machinery to the
899 bacterial pole. *Genes Dev.* **2012**, *26*, 2348–2360.
900183. Dubarry, N.; Willis, C.R.; Ball, G.; Lesterlin, C.; Armitage, J.P. In vivo imaging of the segregation of the 2
901 chromosomes and the cell division proteins of *Rhodobacter sphaeroides* reveals an unexpected role for MipZ.
902 *mBio* **2019**, *10*, e02515–e02518, doi:10.1128/mBio.02515-18.
903184. Toro-Nahuelpan, M.; Corrales-Guerrero, L.; Zwiener, T.; Osorio-Valeriano, M.; Müller, F.-D.; Plitzko, J.M.;
904 Bramkamp, M.; Thanbichler, M.; Schüler, D. A gradient-forming MipZ protein mediating the control of cell
905 division in the magnetotactic bacterium *Magnetospirillum gryphiswaldense*. *Mol. Microbiol.* **2019**, *112*, 1423–
906 1439.
907185. Errington, J.; Wu, L.J. Cell cycle machinery in *Bacillus subtilis*. *Subcell. Biochem.* **2017**, *84*, 67–101.
908186. van Baarle, S.; Bramkamp, M. The MinCDJ system in *Bacillus subtilis* prevents minicell formation by
909 promoting divisome disassembly. *PLoS ONE* **2010**, *5*, e9850, doi:10.1371/journal.pone.0009850.
910187. Sievers, J.; Raether, B.; Perego, M.; Errington, J. Characterization of the *parB*-like *yjaA* gene of *Bacillus*
911 *subtilis*. *J. Bacteriol.* **2002**, *184*, 1102–1111.
912188. Wu, L.J.; Ishikawa, S.; Kawai, Y.; Oshima, T.; Ogasawara, N.; Errington, J. Noc protein binds to specific
913 DNA sequences to coordinate cell division with chromosome segregation. *EMBO J.* **2009**, *28*, 1940–1952.
914189. Adams, D.W.; Wu, L.J.; Errington, J. Nucleoid occlusion protein Noc recruits DNA to the bacterial cell
915 membrane. *EMBO J.* **2015**, *34*, 491–501.

916190. Hajduk, I.V.; Mann, R.; Rodrigues, C.D.A.; Harry, E.J. The ParB homologs, Spo0J and Noc, together prevent
917 premature midcell Z ring assembly when the early stages of replication are blocked in *Bacillus subtilis*. *Mol.*
918 *Microbiol.* **2019**, *112*, 766–784.
919191. Hammond, L.R.; White, M.L.; Eswara, P.J. ¡vIVA la DivIVA! *J. Bacteriol.* **2019**, *201*, e00245-19,
920 doi:10.1128/JB.00245-19.
921192. Bergé, M.; Viollier, P.H. End-in-sight: Cell polarization by the polygenic organizer PopZ. *Trends Microbiol.*
922 **2018**, *26*, 363–375.
923193. Marczynski, G.T.; Petit, K.; Patel, P. Crosstalk regulation between bacterial chromosome replication and
924 chromosome partitioning. *Front. Microbiol.* **2019**, *10*, 279, doi:10.3389/fmicb.2019.00279.
925194. Ausmees, N.; Kuhn, J.R.; Jacobs-Wagner, C. The bacterial cytoskeleton: An intermediate filament-like
926 function in cell shape. *Cell* **2003**, *115*, 705–713.
927195. Refes, Y.; He, B.; Corrales-Guerrero, L.; Steinchen, W.; Panis, G.; Viollier, P.H.; Bange, G.; Thanbichler, M.
928 Molecular architecture of the DNA-binding sites of the P-loop ATPases MipZ and ParA from *Caulobacter*
929 *crenatus*. *bioRxiv* **2019**, 766287, doi:10.1101/766287.
930196. Kiebusch, D.; Michie, K.A.; Essen, L.-O.; Löwe, J.; Thanbichler, M. Localized dimerization and nucleoid
931 binding drive gradient formation by the bacterial cell division inhibitor MipZ. *Mol. Cell* **2012**, *46*, 245–259.
932197. Tettelin, H.; Nelson, K.E.; Paulsen, I.T.; Eisen, J.A.; Read, T.D.; Peterson, S.; Heidelberg, J.; DeBoy, R.T.;
933 Haft, D.H.; Dodson, R.J.; et al. Complete genome sequence of a virulent isolate of *Streptococcus pneumoniae*.
934 *Science* **2001**, *293*, 498–506.
935198. Thomas, C.M.; Smith, C.A.; Shingler, V.; Cross, M.A.; Hussain, A.A.; Pinkney, M. Regulation of replication
936 and maintenance functions of broad host-range plasmid RK2. *Basic Life Sci.* **1985**, *30*, 261–276.
937199. Jagura-Burdzy, G.; Kostelidou, K.; Pole, J.; Khare, D.; Jones, A.; Williams, D.R.; Thomas, C.M. IncC of broad-
938 host-range plasmid RK2 modulates KorB transcriptional repressor activity in vivo and operator binding *in*
939 *vitro*. *J. Bacteriol.* **1999**, *181*, 2807–2815.
940200. Kulinska, A.; Godziszewska, J.; Wojciechowska, A.; Ludwiczak, M.; Jagura-Burdzy, G. Global
941 transcriptional regulation of backbone genes in broad-host-range plasmid RA3 from the IncU group
942 involves segregation protein KorB (ParB family). *Appl. Environ. Microbiol.* **2016**, *82*, 2320–2335.
943201. Bartosik, A.A.; Glabski, K.; Jecz, P.; Mikulska, S.; Fogtman, A.; Koblovska, M.; Jagura-Burdzy, G.
944 Transcriptional profiling of ParA and ParB mutants in actively dividing cells of an opportunistic human
945 pathogen *Pseudomonas aeruginosa*. *PLoS ONE* **2014**, *9*, e87276, doi:10.1371/journal.pone.0087276.
946202. Lasocki, K.; Bartosik, A.A.; Mierzejewska, J.; Thomas, C.M.; Jagura-Burdzy, G. Deletion of the *parA* (*soj*)
947 homologue in *Pseudomonas aeruginosa* causes ParB instability and affects growth rate, chromosome
948 segregation, and motility. *J. Bacteriol.* **2007**, *189*, 5762–5772.
949203. Kawalek, A.; Glabski, K.; Bartosik, A.A.; Fogtman, A.; Jagura-Burdzy, G. Increased ParB level affects
950 expression of stress response, adaptation and virulence operons and potentiates repression of promoters
951 adjacent to the high affinity binding sites *parS3* and *parS4* in *Pseudomonas aeruginosa*. *PLoS ONE* **2017**, *12*,
952 e0181726, doi:10.1371/journal.pone.0181726.
953204. Jun, S.; Wright, A. Entropy as the driver of chromosome segregation. *Nat. Rev. Microbiol.* **2010**, *8*, 600–607.
954205. Jun, S.; Mulder, B. Entropy-driven spatial organization of highly confined polymers: Lessons for the
955 bacterial chromosome. *Proc. Natl. Acad. Sci. USA* **2006**, *103*, 12388–12393.
956206. Weber, P.M.; Moessel, F.; Paredes, G.F.; Viehboeck, T.; Vischer, N.O.E.; Bulgheresi, S. A Bidimensional
957 segregation mode maintains symbiont chromosome orientation toward its host. *Curr. Biol.* **2019**, *29*, 3018–
958 3028.
959207. Jakimowicz, D.; Mouz, S.; Zakrzewska-Czerwinska, J.; Chater, K.F. Developmental control of a *parAB*
960 promoter leads to formation of sporulation-associated ParB complexes in *Streptomyces coelicolor*. *J. Bacteriol.*
961 **2006**, *188*, 1710–1720.
962208. Casart, Y.; Gamero, E.; Rivera-Gutierrez, S.; González-Y.-Merchand, J.A.; Salazar, L. *par* genes in
963 *Mycobacterium bovis* and *Mycobacterium smegmatis* are arranged in an operon transcribed from “SigGC”
964 promoters. *BMC Microbiol.* **2008**, *8*, 51, doi:10.1186/1471-2180-8-51.
965209. Manuse, S.; Fleurie, A.; Zucchini, L.; Lesterlin, C.; Grangeasse, C. Role of eukaryotic-like serine/threonine
966 kinases in bacterial cell division and morphogenesis. *FEMS Microbiol. Rev.* **2016**, *40*, 41–56.
967210. Janczarek, M.; Vinardell, J.-M.; Lipa, P.; Karaś, M. Hanks-type serine/threonine protein kinases and
968 phosphatases in bacteria: Roles in signaling and adaptation to various environments. *Int. J. Mol. Sci.* **2018**,
969 *19*, e2872, doi:10.3390/ijms19102872.

970211. Carabetta, V.J.; Cristea, I.M. Regulation, function, and detection of protein acetylation in bacteria. *J.*
971 *Bacteriol.* **2017**, *199*, e00107–e00117, doi:10.1128/JB.00107-17.
972212. Baronian, G.; Ginda, K.; Berry, L.; Cohen-Gonsaud, M.; Zakrzewska-Czerwińska, J.; Jakimowicz, D.; Molle,
973 V. Phosphorylation of *Mycobacterium tuberculosis* ParB participates in regulating the ParABS chromosome
974 segregation system. *PLoS ONE* **2015**, *10*, e0119907, doi:10.1371/journal.pone.0119907.
975213. Chawla, Y.; Upadhyay, S.; Khan, S.; Nagarajan, S.N.; Forti, F.; Nandicoori, V.K. Protein kinase B (PknB) of
976 *Mycobacterium tuberculosis* is essential for growth of the pathogen *in vitro* as well as for survival within the
977 host. *J. Biol. Chem.* **2014**, *289*, 13858–13875.



© 2020 by the authors. Licensee MDPI, Basel, Switzerland. This article is an open access article distributed under the terms and conditions of the Creative Commons Attribution (CC BY) license (<http://creativecommons.org/licenses/by/4.0/>).

978

979